

CONVERGENCE OF LAGRANGE FINITE ELEMENTS FOR THE MAXWELL EIGENVALUE PROBLEM IN 2D

DANIELE BOFFI, JOHNNY GUZMÁN, AND MICHAEL NEILAN

ABSTRACT. We consider finite element approximations of the Maxwell eigenvalue problem in two dimensions. We prove, in certain settings, convergence of the discrete eigenvalues using Lagrange finite elements. In particular, we prove convergence in three scenarios: piecewise linear elements on Powell–Sabin triangulations, piecewise quadratic elements on Clough–Tocher triangulations, and piecewise quartics (and higher) elements on general shape-regular triangulations. We provide numerical experiments that support the theoretical results. The computations also show that, on general triangulations, the eigenvalue approximations are very sensitive to nearly singular vertices, i.e., vertices that fall on exactly two “almost” straight lines.

1. INTRODUCTION

Let $\Omega \subset \mathbb{R}^2$ be a contractible polygonal domain and consider the eigenvalue problem: Find $\mathbf{u} \in \mathbf{H}_0(\text{rot}, \Omega)$ such that

$$(1.1) \quad (\text{rot } \mathbf{u}, \text{rot } \mathbf{v}) = \eta^2(\mathbf{u}, \mathbf{v}) \quad \forall \mathbf{v} \in \mathbf{H}_0(\text{rot}, \Omega),$$

where $\mathbf{H}(\text{rot}, \Omega) := \{\mathbf{v} \in \mathbf{L}^2(\Omega) : \text{rot } \mathbf{v} \in L^2(\Omega)\}$, $\mathbf{H}_0(\text{rot}, \Omega) := \{\mathbf{v} \in \mathbf{H}(\text{rot}, \Omega) : \mathbf{v} \cdot \mathbf{t} = 0 \text{ on } \partial\Omega\}$, and (\cdot, \cdot) denotes the L^2 inner product over Ω . Given a finite element space $\mathring{\mathbf{V}}_h \subset \mathbf{H}_0(\text{rot}, \Omega)$, a finite element method seeks $\mathbf{u}_h \in \mathring{\mathbf{V}}_h \setminus \{0\}$ and $\eta_h \in \mathbb{R}$ satisfying

$$(1.2) \quad (\text{rot } \mathbf{u}_h, \text{rot } \mathbf{v}_h) = \eta_h^2(\mathbf{u}_h, \mathbf{v}_h) \quad \forall \mathbf{v}_h \in \mathring{\mathbf{V}}_h.$$

For example, one can take $\mathring{\mathbf{V}}_h$ to be the $\mathbf{H}_0(\text{rot}; \Omega)$ -conforming Nédélec finite elements (i.e., the rotated Raviart-Thomas finite elements) as the finite element space. It is well-known this choice leads to a convergent approximation of the eigenvalue problem. On the other hand, taking $\mathring{\mathbf{V}}_h$ as a space of continuous piecewise polynomials (i.e., a $\mathbf{H}^1(\Omega)$ -conforming Lagrange finite element) may lead to spurious eigenvalues for any mesh parameter.

There is a vast literature on this subject. The interested reader is referred to [8, Section 20] for an extensive survey including a comprehensive list of references about Nédélec finite elements and to [11, 9] for a discussion about the use of standard Lagrange finite elements (see also [3] for a discussion of these phenomena in the context of the finite element exterior calculus). Many formulations have been developed based on penalization and/or regularization (e.g., [19, 13, 12, 6, 23, 24, 22]), showing Lagrange elements can lead to consistent approximations to (1.1). However, we are not aware of a previous analysis of Lagrange elements on macro elements using the standard formulation (1.2), and this is the main objective of this work.

To better appreciate the problem and its discretization, we consider the equivalent formulation introduced in [11] for $\eta \neq 0$: $(\boldsymbol{\sigma}, p) \in \mathbf{H}_0(\text{rot}, \Omega) \times L_0^2(\Omega)$ such that

$$(1.3a) \quad (\boldsymbol{\sigma}, \boldsymbol{\tau}) + (p, \text{rot } \boldsymbol{\tau}) = 0 \quad \forall \boldsymbol{\tau} \in \mathbf{H}_0(\text{rot}, \Omega),$$

$$(1.3b) \quad (\text{rot } \boldsymbol{\sigma}, q) = -\lambda(p, q) \quad \forall q \in L_0^2(\Omega).$$

The first author is a member of the INdAM Research group GNCS and his research is partially supported by IMATI/CNR and by PRIN/MIUR. The second author is partially supported by the NSF grant DMS-1620100. The third author is partially supported by the NSF grants DMS-1719829 and DMS-2011733.

Taking $q = \text{rot } \mathbf{v}$ with $\mathbf{v} \in \mathbf{H}_0(\text{rot}, \Omega)$ shows the equivalence of (1.3) and (1.1) with $\boldsymbol{\sigma} = \mathbf{u}$, $\lambda = \eta^2$, and $p = -\frac{1}{\lambda} \text{rot } \mathbf{u}$.

The corresponding finite element method for the mixed formulation (1.3) seeks $\boldsymbol{\sigma}_h \in \mathring{\mathbf{V}}_h \setminus \{0\}$, $p_h \in \mathring{Q}_h$, and $\lambda_h \in \mathbb{R}$ such that

$$(1.4a) \quad (\boldsymbol{\sigma}_h, \boldsymbol{\tau}_h) + (p_h, \text{rot } \boldsymbol{\tau}_h) = 0, \quad \forall \boldsymbol{\tau}_h \in \mathring{\mathbf{V}}_h,$$

$$(1.4b) \quad (\text{rot } \boldsymbol{\sigma}_h, q_h) = -\lambda_h(p_h, q_h) \quad \forall q_h \in \mathring{Q}_h$$

with $\mathring{Q}_h \subset L_0^2(\Omega)$. Similar to the continuous problem, if the finite element spaces satisfy $\text{rot } \mathring{\mathbf{V}}_h \subset \mathring{Q}_h$, then the mixed finite element formulation (1.4) is equivalent to the primal one (1.2) with $\boldsymbol{\sigma}_h = \mathbf{u}_h$, $\lambda_h = \eta_h^2$ and $p_h = -\frac{1}{\lambda_h} \text{rot } \mathbf{u}_h$.

If $\mathring{\mathbf{V}}_h$ is the Nédélec space of index k , then we may take \mathring{Q}_h to be the space of piecewise polynomials of degree $k-1$. In this case, $(\mathring{\mathbf{V}}_h, \mathring{Q}_h)$ forms an inf-sup stable pair of spaces, in particular, there exists a Fortin projection

$$\mathbf{\Pi}_V : \mathring{\mathbf{V}} \rightarrow \mathring{\mathbf{V}}_h$$

satisfying

$$(1.5a) \quad \text{rot } \mathbf{\Pi}_V \boldsymbol{\tau} = \mathbf{\Pi}_Q \text{rot } \boldsymbol{\tau} \quad \forall \boldsymbol{\tau} \in \mathring{\mathbf{V}},$$

$$(1.5b) \quad \|\mathbf{\Pi}_V \boldsymbol{\tau} - \boldsymbol{\tau}\|_{L^2(\Omega)} \leq Ch^{\frac{1}{2}+\delta} (\|\boldsymbol{\tau}\|_{H^{\frac{1}{2}+\delta}(\Omega)} + \|\text{rot } \boldsymbol{\tau}\|_{L^2(\Omega)}) \quad \forall \boldsymbol{\tau} \in \mathring{\mathbf{V}}.$$

Here $\mathring{\mathbf{V}} := \mathbf{H}_0(\text{rot}, \Omega) \cap \mathbf{H}(\text{div}, \Omega)$. Moreover, $\delta \in (0, \frac{1}{2}]$ is a parameter such that $\mathring{\mathbf{V}} \hookrightarrow \mathbf{H}^{\frac{1}{2}+\delta}(\Omega)$ [2], and $\mathbf{\Pi}_Q : L_0^2(\Omega) \rightarrow \mathring{Q}_h$ is the L^2 orthogonal projection onto \mathring{Q}_h . Using this projection one can prove that the corresponding source problems converges uniformly, and this is sufficient to prove convergence of the eigenvalue problem (1.2) (see [32, 8] and Proposition 2.1).

On the other hand, if $\mathring{\mathbf{V}}_h$ is taken to be the Lagrange finite element space of degree k , then a natural choice of \mathring{Q}_h is the space of (discontinuous) piecewise polynomials of degree $k-1$. However, $(\mathring{\mathbf{V}}_h, \mathring{Q}_h)$ is *not* inf-sup stable on generic triangulations, at least when $k=1$ [39, 10], and therefore there does not exist a Fortin projection satisfying (1.5). On the other hand, the pair $(\mathring{\mathbf{V}}_h, \mathring{Q}_h)$ is known to be stable on special triangulations, even if the inf-sup condition might not be sufficient to guarantee the existence of a Fortin projector satisfying (1.5) (see [9]).

Wong and Cendes [42] showed numerically that, on very special triangulations, solutions to (1.2) do converge to the correct eigenvalues using piecewise linear Lagrange elements (i.e., $k=1$). In fact, they used precisely the Powell–Sabin triangulations (see Figure 1). A rigorous proof of this result has remained unsettled until now; see the review paper [8] for a discussion. Specifically, we prove that using Lagrange elements in conjunction with Powell–Sabin triangulation leads to a convergent method. We do this by proving that there is a Fortin projection of sorts. We show that there exists an operator $\mathbf{\Pi}_V : \mathring{\mathbf{V}}(Q_h) \rightarrow \mathring{\mathbf{V}}_h$ satisfying

$$(1.6a) \quad \text{rot } \mathbf{\Pi}_V \boldsymbol{\tau} = \text{rot } \boldsymbol{\tau} \quad \forall \boldsymbol{\tau} \in \mathring{\mathbf{V}}(Q_h),$$

$$(1.6b) \quad \|\mathbf{\Pi}_V \boldsymbol{\tau} - \boldsymbol{\tau}\|_{L^2(\Omega)} \leq Ch^{\frac{1}{2}+\delta} (\|\boldsymbol{\tau}\|_{H^{\frac{1}{2}+\delta}(\Omega)} + \|\text{rot } \boldsymbol{\tau}\|_{L^2(\Omega)}), \quad \forall \boldsymbol{\tau} \in \mathring{\mathbf{V}}(Q_h),$$

where $\mathring{\mathbf{V}}(Q_h) = \{\mathbf{v} \in \mathring{\mathbf{V}} : \text{rot } \mathbf{v} \in \mathring{Q}_h\}$. Note that (1.5) implies (1.6), and we prove convergence of the eigenvalue problem whenever there is a projection $\mathbf{\Pi}_V$ satisfying (1.6). In addition to linear Lagrange elements on Powell–Sabin triangulations, we prove the existence of such a projection on Clough–Tocher splits using quadratic Lagrange elements, and on general triangulations using k th degree Lagrange elements with $k \geq 4$ (i.e., the Scott–Vogelius finite elements). For the Scott–Vogelius finite elements, we find the approximate eigenvalues are extremely sensitive if the mesh has nearly singular vertices, i.e., vertices that fall on exactly two “almost” straight lines (cf. Section 3.3). We give numerical examples that illustrate this behavior.

The analysis of composite triangulations (e.g. Clough-Tocher and Powell-Sabin) on the problem (1.1) goes back at least to the work of Costabel and Dauge [19]. Recently, Duan et al. [23, 24, 22]

considered Lagrange finite elements for Maxwell's eigenvalue problem in two and three dimensions using composite triangulations. However, as noted earlier, they use a different formulation than the standard one (1.2). In particular, in [22] they add a Lagrange multiplier and an equation of the form appears $(\operatorname{div} \mathbf{u}_h, q_h) = 0$ which can be thought of as a Kikuchi-type formulation [33], where one transfers the derivatives to \mathbf{u}_h . In [24] a similar formulation is used with a regularization term.

As mentioned above, the main idea to show convergence of Lagrange elements using the standard formulation (1.1) on certain triangulations is the construction of a Fortin-type operation with certain approximation properties. On certain composite triangulations (e.g. Powell-Sabin, Clough-Tocher, Alfeld, Worsey-Farin) exact sequences and/or Fortin projections have been developed; see for example [29, 30, 28, 43, 39, 14]. These results have led to stable finite element for fluid flow problems; see for example [35]. In this paper, for the Powell-Sabin and Clough-Tocher triangulations, we cannot directly use the Fortin projections defined in [29, 28] since they require too much smoothness. Instead, we pre-process with a Scott-Zhang type interpolant that preserves the vanishing tangential components, and then use the degrees of freedom in [29, 28]. These projections are sufficient for our purposes, however, it would be very interesting to see if one can construct L^2 bounded commuting projection for these sequences as is done in the finite element exterior calculus (FEEC) [15]. If bounded L^2 bounded commuting projections exist, then the convergence of eigenvalue problems follows from the general theory in FEEC [4, 3, 8].

The paper is organized as follows: In the next section we give a convergence proof for finite elements spaces with stable projections. In Section 3, we provide three examples of Lagrange finite element spaces with stable projections: the piecewise linear Lagrange space on Powell-Sabin splits, the piecewise quadratic Lagrange space on Clough-Tocher splits, and the piecewise k th degree Lagrange space on generic triangulations. In Section 4 we provide numerical experiments and make some concluding remarks in Section 5.

2. CONVERGENCE FRAMEWORK

Define the two-dimensional **curl**, **rot**, and divergence operators as

$$\mathbf{curl} u = \left(\frac{\partial u}{\partial x_2}, -\frac{\partial u}{\partial x_1} \right)^\top, \quad \operatorname{rot} \mathbf{v} = \frac{\partial v_2}{\partial x_1} - \frac{\partial v_1}{\partial x_2}, \quad \operatorname{div} \mathbf{v} = \frac{\partial v_1}{\partial x_1} + \frac{\partial v_2}{\partial x_2},$$

and define the Hilbert spaces

$$\begin{aligned} \mathbf{H}_0(\operatorname{rot}, \Omega) &= \{ \mathbf{v} \in \mathbf{L}^2(\Omega) : \operatorname{rot} \mathbf{v} \in L^2(\Omega), \mathbf{v} \cdot \mathbf{t}|_{\partial\Omega} = 0 \}, \\ \mathbf{H}(\operatorname{div}, \Omega) &= \{ \mathbf{v} \in \mathbf{L}^2(\Omega) : \operatorname{div} \mathbf{v} \in L^2(\Omega) \}, \end{aligned}$$

where \mathbf{t} is a unit tangent vector of $\partial\Omega$. Recall that $\mathring{\mathbf{V}} = \mathbf{H}_0(\operatorname{rot}, \Omega) \cap \mathbf{H}(\operatorname{div}, \Omega)$.

Let $\mathring{\mathbf{V}}_h \subset \mathbf{H}_0(\operatorname{rot}, \Omega)$ and $\mathring{Q}_h \subset L_0^2(\Omega)$ be finite element spaces such that $\operatorname{rot} \mathring{\mathbf{V}}_h \subset \mathring{Q}_h$.

2.1. Source problems. We will require the corresponding source problems for the analysis. To this end, we define the solution operators $\mathbf{A} : L^2(\Omega) \rightarrow \mathbf{H}_0(\operatorname{rot}, \Omega)$ and $T : L^2(\Omega) \rightarrow L_0^2(\Omega)$ such that for given $f \in L^2(\Omega)$, there holds

$$(2.1a) \quad (\mathbf{A}f, \boldsymbol{\tau}) + (Tf, \operatorname{rot} \boldsymbol{\tau}) = 0, \quad \forall \boldsymbol{\tau} \in \mathbf{H}_0(\operatorname{rot}, \Omega),$$

$$(2.1b) \quad (\operatorname{rot} \mathbf{A}f, q) = (f, q) \quad \forall q \in L_0^2(\Omega).$$

Likewise, the discrete source problem is given by: Find $\mathbf{A}_h f \in \mathring{\mathbf{V}}_h$ and $T_h f \in \mathring{Q}_h$ such that

$$(2.2a) \quad (\mathbf{A}_h f, \boldsymbol{\tau}_h) + (T_h f, \operatorname{rot} \boldsymbol{\tau}_h) = 0 \quad \forall \boldsymbol{\tau}_h \in \mathring{\mathbf{V}}_h,$$

$$(2.2b) \quad (\operatorname{rot} \mathbf{A}_h f, q_h) = (f, q_h) \quad \forall q_h \in \mathring{Q}_h.$$

Note that $\mathbf{A}f = \mathbf{curl} Tf$, and so $\operatorname{div} \mathbf{A}f = 0$. Moreover, using that $\operatorname{rot} \mathbf{A}f = f$ we have that $\mathbf{A}f \in \mathring{\mathbf{V}}$.

We define the operator norm:

$$(2.3) \quad \|T - T_h\| := \sup_{f \in L^2(\Omega) \setminus \{0\}} \frac{\|(T - T_h)f\|_{L^2(\Omega)}}{\|f\|_{L^2(\Omega)}}.$$

We will use the next standard result that states that the uniform convergence of the discrete source problem implies convergence of the discrete eigenvalues. This result is a consequence of the classical discussion in [5, Section 8] (see also [8, Section 9] and [11, Theorem 4.4]).

Proposition 2.1. *Let T and T_h be defined from (2.1) and (2.2), respectively, and suppose that $\|T - T_h\| \rightarrow 0$ as $h \rightarrow 0$. Consider the problem (1.3) and consider the nonzero eigenvalues $0 < \lambda^{(1)} \leq \lambda^{(2)} \leq \dots$. Consider also (1.4) and its non-zero eigenvalues $0 < \lambda_h^{(1)} \leq \lambda_h^{(2)} \leq \dots$. Then, for any fixed i , $\lim_{h \rightarrow 0} \lambda_h^{(i)} = \lambda^{(i)}$.*

Therefore, to prove convergence of eigenvalues it suffices to show uniform convergence of the discrete source problem. To prove this, we will exploit the embedding $\mathring{\mathbf{V}} \hookrightarrow \mathbf{H}^{\frac{1}{2}+\delta}(\Omega)$ along with an assumption on the finite element spaces. The embedding result is proved in three dimensions in [2], and we state the two dimensional version here.

Proposition 2.2. *Let Ω be a contractible polygonal domain. Then there exists constants $\delta \in (0, \frac{1}{2}]$ and $C > 0$ such that*

$$\|\mathbf{v}\|_{\mathbf{H}^{\frac{1}{2}+\delta}(\Omega)} \leq C(\|\operatorname{div} \mathbf{v}\|_{L^2(\Omega)} + \|\operatorname{rot} \mathbf{v}\|_{L^2(\Omega)}) \quad \forall \mathbf{v} \in \mathring{\mathbf{V}}.$$

From now on δ will refer to the delta of the above proposition. We will use the following space

$$(2.4) \quad \mathring{\mathbf{V}}(Q_h) = \{\boldsymbol{\tau} \in \mathring{\mathbf{V}} : \operatorname{rot} \boldsymbol{\tau} \in \mathring{Q}_h\}.$$

Assumption 2.3. *We assume that $\operatorname{rot} \mathring{\mathbf{V}}_h \subset \mathring{Q}_h$ and the existence of a projection $\mathbf{\Pi}_V : \mathring{\mathbf{V}}(Q_h) \rightarrow \mathring{\mathbf{V}}_h$ such that*

$$(2.5a) \quad \operatorname{rot} \mathbf{\Pi}_V \boldsymbol{\tau} = \operatorname{rot} \boldsymbol{\tau} \quad \forall \boldsymbol{\tau} \in \mathring{\mathbf{V}}(Q_h),$$

$$(2.5b) \quad \|\mathbf{\Pi}_V \boldsymbol{\tau} - \boldsymbol{\tau}\|_{L^2(\Omega)} \leq \omega_0(h)(\|\boldsymbol{\tau}\|_{\mathbf{H}^{\frac{1}{2}+\delta}(\Omega)} + \|\operatorname{rot} \boldsymbol{\tau}\|_{L^2(\Omega)}) \quad \forall \boldsymbol{\tau} \in \mathring{\mathbf{V}}(Q_h).$$

Furthermore, we assume that the L^2 -orthogonal projection $\mathbf{\Pi}_Q : L^2(\Omega) \rightarrow \mathring{Q}_h$ satisfies

$$\|\mathbf{\Pi}_Q \phi - \phi\|_{L^2(\Omega)} \leq \omega_1(h) \|\operatorname{curl} \phi\|_{L^2(\Omega)} \quad \forall \phi \in H^1(\Omega) \cap L_0^2(\Omega).$$

Here, the constants are assumed to satisfy $\omega_0(h), \omega_1(h) > 0$ and $\lim_{h \rightarrow 0^+} \omega_i(h) = 0$ for $i = 0, 1$.

Theorem 2.4. *Suppose that $(\mathring{\mathbf{V}}_h, \mathring{Q}_h)$ satisfy Assumption 2.3. Let T and T_h be defined by (2.1) and (2.2), respectively. Then there holds*

$$\|T - T_h\| \leq C(\omega_0(h) + \omega_1(h)).$$

Note that Theorem 2.4 and Proposition 2.1 imply that the discrete eigenvalues in the finite element method (1.2) converge to the correct values. To prove Theorem 2.4, we require two preliminary results.

Lemma 2.5. *Suppose that Assumption 2.3 is satisfied. Then there exists a constant $C > 0$ such that*

$$\|\mathbf{A}\mathbf{\Pi}_Q f - \mathbf{A}f\|_{L^2(\Omega)} + \|T\mathbf{\Pi}_Q f - Tf\|_{L^2(\Omega)} \leq C\omega_1(h)\|f\|_{L^2(\Omega)} \quad \forall f \in L^2(\Omega).$$

Proof. Let $f \in L^2(\Omega)$ and set $\boldsymbol{\sigma} = \mathbf{A}f, u = Tf, \boldsymbol{\psi} = \mathbf{A}\mathbf{\Pi}_Q f$ and $w = T\mathbf{\Pi}_Q f$. We see that

$$(2.6a) \quad (\boldsymbol{\sigma} - \boldsymbol{\psi}, \boldsymbol{\tau}) + (u - w, \operatorname{rot} \boldsymbol{\tau}) = 0 \quad \forall \boldsymbol{\tau} \in \mathbf{H}_0(\operatorname{rot}, \Omega),$$

$$(2.6b) \quad (\operatorname{rot}(\boldsymbol{\sigma} - \boldsymbol{\psi}), v) = (f - \mathbf{\Pi}_Q f, v) \quad \forall v \in L_0^2(\Omega).$$

Setting $v = w - u$ in (2.6b) and $\boldsymbol{\tau} = \boldsymbol{\sigma} - \boldsymbol{\psi}$ in (2.6a), and adding the result yields $\|\boldsymbol{\sigma} - \boldsymbol{\psi}\|_{L^2(\Omega)}^2 = (f - \mathbf{\Pi}_Q f, w - u)$. Furthermore, (2.6a) implies $\operatorname{curl}(u - w) = \boldsymbol{\sigma} - \boldsymbol{\psi}$. Therefore, there holds

$$\|\boldsymbol{\sigma} - \boldsymbol{\psi}\|_{L^2(\Omega)} \leq \sup_{\phi \in H^1(\Omega) \cap L_0^2(\Omega)} \frac{(f - \mathbf{\Pi}_Q f, \phi)}{\|\operatorname{curl} \phi\|_{L^2(\Omega)}}.$$

However, the properties of the L^2 projection and Assumption 2.3 give us

$$\sup_{\phi \in H^1(\Omega) \cap L_0^2(\Omega)} \frac{(f - \Pi_Q f, \phi)}{\|\mathbf{curl} \phi\|_{L^2(\Omega)}} = \sup_{\phi \in H^1(\Omega) \cap L_0^2(\Omega)} \frac{(f, \phi - \Pi_Q \phi)}{\|\mathbf{curl} \phi\|_{L^2(\Omega)}} \leq \omega_1(h) \|f\|_{L^2(\Omega)}.$$

Thus, we have shown

$$\|\mathbf{A}\Pi_Q f - \mathbf{A}f\|_{L^2(\Omega)} \leq \omega_1(h) \|f\|_{L^2(\Omega)}.$$

Finally, because $Tf \in L_0^2(\Omega)$, we have by the Poincare inequality

$$\|T\Pi_Q f - Tf\|_{L^2(\Omega)} \leq C \|\mathbf{curl}(T\Pi_Q f - Tf)\|_{L^2(\Omega)} = \|\mathbf{A}\Pi_Q f - \mathbf{A}f\|_{L^2(\Omega)} \leq C\omega_1(h) \|f\|_{L^2(\Omega)}. \quad \square$$

Next we prove that Assumption 2.3 implies the inf-sup condition for the pair $(\mathring{\mathbf{V}}_h, \mathring{Q}_h)$.

Lemma 2.6. *Suppose that Assumption 2.3 is satisfied. Then there exists a constant $C > 0$ such that for every $u_h \in \mathring{Q}_h$, there exists $\tau_h \in \mathring{\mathbf{V}}_h$ such that $\text{rot } \tau_h = u_h$ and $\|\tau_h\|_{L^2(\Omega)} \leq C \|u_h\|_{L^2(\Omega)}$.*

Proof. Let $\tau \in \mathbf{H}_0^1(\Omega)$ with $\text{rot } \tau = u_h$ such that $\|\tau\|_{H^1(\Omega)} \leq C \|u_h\|_{L^2(\Omega)}$. Noting that $\tau \in \mathring{\mathbf{V}}(Q_h)$, we define $\tau_h = \mathbf{\Pi}_V \tau$ so that $\text{rot } \tau_h = \text{rot } \tau = u_h$. Moreover,

$$\|\tau_h\|_{L^2(\Omega)} \leq C(\|\tau\|_{H^{\frac{1}{2}+\delta}(\Omega)} + \|\text{rot } \tau\|_{L^2(\Omega)}) \leq C\|\tau\|_{H^1(\Omega)} \leq C\|u_h\|_{L^2(\Omega)}. \quad \square$$

Now we can prove Theorem 2.4.

Proof of Theorem 2.4. Let $f \in L^2(\Omega)$, and set $\sigma = \mathbf{A}f$, $u = Tf$ and $\sigma_h = \mathbf{A}_h f$, $u_h = T_h f$. Let $\psi = \mathbf{A}\Pi_Q f$ and $w = T\Pi_Q f$.

We first derive an estimate for $\psi - \sigma_h$. Using the inclusion $\text{rot } \mathring{\mathbf{V}}_h \subset \mathring{Q}_h$, we see that

$$\begin{aligned} (\mathbf{\Pi}_V \psi - \sigma_h, \tau_h) + (\Pi_Q w - u_h, \text{rot } \tau_h) &= (\mathbf{\Pi}_V \psi - \psi, \tau_h) \quad \forall \tau_h \in \mathring{\mathbf{V}}_h, \\ (\text{rot } (\mathbf{\Pi}_V \psi - \sigma_h), v_h) &= 0 \quad \forall v_h \in \mathring{Q}_h. \end{aligned}$$

Setting $\tau_h = \mathbf{\Pi}_V \psi - \sigma_h$ and applying the Cauchy–Schwarz inequality yields

$$\|\mathbf{\Pi}_V \psi - \sigma_h\|_{L^2(\Omega)} \leq \|\mathbf{\Pi}_V \psi - \psi\|_{L^2(\Omega)} \leq \omega_0(h) (\|\psi\|_{H^{\frac{1}{2}+\delta}(\Omega)} + \|\text{rot } \psi\|_{L^2(\Omega)}).$$

If we use Proposition 2.2 we get

$$\|\psi\|_{H^{\frac{1}{2}+\delta}(\Omega)} \leq C(\|\text{div } \psi\|_{L^2(\Omega)} + \|\text{rot } \psi\|_{L^2(\Omega)}) = C\|\text{rot } \psi\|_{L^2(\Omega)} = C\|\Pi_Q f\|_{L^2(\Omega)} \leq C\|f\|_{L^2(\Omega)}.$$

Hence,

$$\|\mathbf{\Pi}_V \psi - \sigma_h\|_{L^2(\Omega)} \leq C\omega_0(h) \|f\|_{L^2(\Omega)}.$$

Next, we note that by Lemma 2.5,

$$\|\sigma - \psi\|_{L^2(\Omega)} + \|w - u\|_{L^2(\Omega)} \leq C\omega_1(h) \|f\|_{L^2(\Omega)},$$

and therefore,

$$\begin{aligned} \|(\mathbf{A} - \mathbf{A}_h)f\|_{L^2(\Omega)} &= \|\sigma - \sigma_h\|_{L^2(\Omega)} \\ &\leq \|\sigma - \psi\|_{L^2(\Omega)} + \|\sigma_h - \mathbf{\Pi}_V \psi\|_{L^2(\Omega)} + \|\mathbf{\Pi}_V \psi - \psi\|_{L^2(\Omega)} \\ &\leq C(\omega_0(h) + \omega_1(h)) \|f\|_{L^2(\Omega)}. \end{aligned}$$

Using the inf-sup stability stated in Lemma 2.6, we have

$$\|\Pi_Q w - u_h\|_{L^2(\Omega)} \leq C\|\psi - \sigma_h\|_{L^2(\Omega)} \leq C(\omega_0(h) + \omega_1(h)) \|f\|_{L^2(\Omega)}.$$

Hence, we have

$$\begin{aligned} \|w - u_h\|_{L^2(\Omega)} &\leq C(\omega_0(h) + \omega_1(h)) \|f\|_{L^2(\Omega)} + \|w - \Pi_Q w\|_{L^2(\Omega)} \\ &\leq C(\omega_0(h) + \omega_1(h)) \|f\|_{L^2(\Omega)} + \omega_1(h) \|\mathbf{curl} w\|_{L^2(\Omega)}. \end{aligned}$$

But we have $\|\mathbf{curl} w\|_{L^2(\Omega)} \leq C\|\Pi_Q f\|_{L^2(\Omega)} \leq C\|f\|_{L^2(\Omega)}$, and so

$$\|(T - T_h)f\|_{L^2(\Omega)} = \|u - u_h\|_{L^2(\Omega)} \leq C(\omega_0(h) + \omega_1(h))\|f\|_{L^2(\Omega)}.$$

□

3. EXAMPLES OF FORTIN OPERATORS

In this section we give examples of finite element pairs satisfying Assumption 2.3, where $\mathring{\mathbf{V}}_h$ is taken to be a space of continuous, piecewise polynomials, i.e., a Lagrange finite element space. Here we use recent results on divergence-free finite element pairs for the Stokes problem to construct a Fortin projection satisfying (2.5). A common theme of these Stokes pairs is the imposition of mesh conditions for low-polynomial degree finite element spaces; it is well-known that Assumption 2.3 is not satisfied on general simplicial meshes and for low polynomial degree. Before continuing, we introduce some notation.

We denote by \mathcal{T}_h a shape-regular, simplicial triangulation of Ω with $h_T = \text{diam}(T)$ for all $T \in \mathcal{T}_h$, and $h = \max_{T \in \mathcal{T}_h} h_T$. Let $\mathcal{V}_h^I, \mathcal{V}_h^B, \mathcal{V}_h^C$ denote the sets of interior vertices, boundary vertices, and corner vertices, respectively. Note that the cardinality of \mathcal{V}_h^C is uniformly bounded due to the shape-regularity of \mathcal{T}_h . The set of all vertices is $\mathcal{V}_h = \mathcal{V}_h^I \cup \mathcal{V}_h^B$. Likewise, \mathcal{E}_h^I and \mathcal{E}_h^B are the sets of interior and boundary edges, respectively, and $\mathcal{E}_h = \mathcal{E}_h^I \cup \mathcal{E}_h^B$. We denote by $\mathcal{T}_h(z)$ the patch of triangles that have $z \in \mathcal{V}_h$ as a vertex. Likewise, $\mathcal{V}_h^I(T)$ and $\mathcal{V}_h^B(T)$ are the sets of interior and boundary vertices of $T \in \mathcal{T}_h$, and $\mathcal{E}_h^I(T)$ is the set of interior edges of T .

For a non-negative integer k and set $S \subset \Omega$, let $\mathcal{P}_k(S)$ to be the space of piecewise polynomials of degree $\leq k$ with domain S . The analogous space of piecewise polynomials with respect to \mathcal{T}_h is

$$\mathcal{P}_k(\mathcal{T}_h) = \prod_{T \in \mathcal{T}_h} \mathcal{P}_k(T),$$

and the Lagrange finite element space is

$$\mathcal{P}_k^c(\mathcal{T}_h) = \mathcal{P}_k(\mathcal{T}_h) \cap H^1(\Omega).$$

Analogous vector-valued spaces are denoted in boldface, e.g., $\mathbf{P}_k(\mathcal{T}_h) = [\mathcal{P}_k(\mathcal{T}_h)]^2$. Finally, the constant C denotes a generic constant that is independent of the mesh parameter h and may take different values at different occurrences.

In the subsequent sections, we will employ a Scott–Zhang type interpolant on the space $\mathring{\mathbf{V}}$. We cannot use the Scott–Zhang interpolant directly, as the canonical Scott–Zhang interpolant of a function in $\mathring{\mathbf{V}}$ might not have zero tangential components at the corners of Ω ; hence, we have to modify the Scott–Zhang interpolant at the corners of Ω . This type of interpolant has been used for example in [12, (2.14) and (2.15)]. For completeness we give a detailed construction in the appendix but we state the result here.

Lemma 3.1. *Let $0 < \delta \leq \frac{1}{2}$. There exists a projection $\mathbf{I}_h : \mathbf{H}^{\frac{1}{2}+\delta}(\Omega) \cap \mathbf{H}_0(\text{rot}, \Omega) \rightarrow \mathbf{P}_1^c(\mathcal{T}_h) \cap \mathbf{H}_0(\text{rot}, \Omega)$ with the following bound:*

$$(3.1) \quad h_T^{-\frac{1}{2}-\delta} \|\boldsymbol{\tau} - \mathbf{I}_h \boldsymbol{\tau}\|_{L^2(T)} + \|\mathbf{I}_h \boldsymbol{\tau}\|_{H^{\frac{1}{2}+\delta}(T)} \leq C \|\boldsymbol{\tau}\|_{H^{\frac{1}{2}+\delta}(\omega(T))} \quad \forall \boldsymbol{\tau} \in \mathring{\mathbf{V}},$$

where $\omega(T) = \bigcup_{\substack{T' \in \mathcal{T}_h \\ \bar{T} \cap \bar{T}' \neq \emptyset}} T'$.

3.1. Construction of Fortin Operator on Powell–Sabin Splits. In this section, we use the recent results given in [29] to construct a Fortin projection into the Lagrange finite element space defined on Powell–Sabin triangulations. For simplicity and readability, we focus on the lowest-order case; however, the arguments easily extend to arbitrary polynomial degree $k \geq 1$.

Given the simplicial triangulation of \mathcal{T}_h of Ω , we construct its Powell–Sabin refinement $\mathcal{T}_h^{\text{ps}}$ as follows [38, 34, 29]: First, adjoin the incenter of each $T \in \mathcal{T}_h$ to each vertex of T . Next, the interior

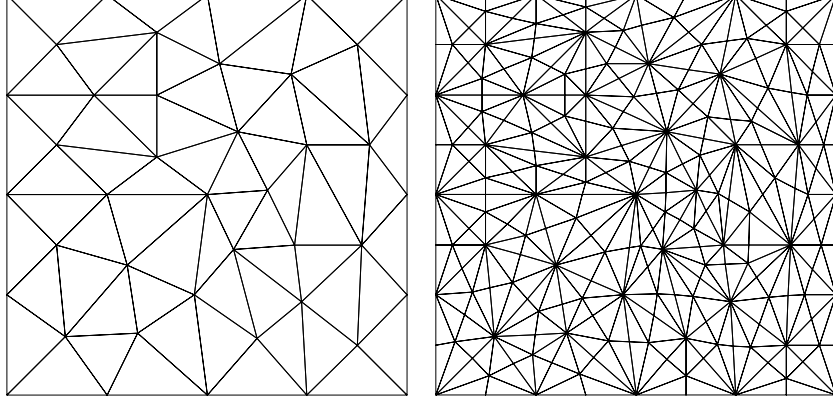


FIGURE 1. A simplicial triangulation of the unit square (left) and the associated Powell–Sabin triangulation (right).

points (incenters) of each adjacent pair of triangles are connected with an edge. For any T that shares an edge with the boundary of Ω , the midpoint of that edge is connected with the incenter of T . Thus, each $T \in \mathcal{T}_h$ is split into six triangles; cf. Figure 1.

Let $\mathcal{S}_h^I(\mathcal{T}_h^{\text{ps}})$ be the points of intersection of the interior edges of \mathcal{T}_h that adjoin incenters, let $\mathcal{S}_h^B(\mathcal{T}_h^{\text{ps}})$ be the intersection points of the boundary edges that adjoin incenters, and set $\mathcal{S}_h(\mathcal{T}_h^{\text{ps}}) = \mathcal{S}_h^I(\mathcal{T}_h^{\text{ps}}) \cup \mathcal{S}_h^B(\mathcal{T}_h^{\text{ps}})$. Note that, by the definition of the Powell–Sabin split, the points in $\mathcal{S}_h(\mathcal{T}_h^{\text{ps}})$ are the singular vertices in $\mathcal{T}_h^{\text{ps}}$, i.e., the vertices that lie on exactly two straight lines. In particular, for a vertex $z \in \mathcal{S}_h^I(\mathcal{T}_h^{\text{ps}})$ there exists four triangles $\mathcal{T}_h^{\text{ps}}(z) = \{T_i\}_{i=1}^4 \subset \mathcal{T}_h^{\text{ps}}$ such that z is a vertex of T_i . Without loss of generality we assume that these triangles are labeled in a counterclockwise direction. We then define for a scalar function v ,

$$(3.2) \quad \theta_z(v) := v|_{T_1}(z) - v|_{T_2}(z) + v|_{T_3}(z) - v|_{T_4}(z).$$

We then define the spaces

$$(3.3a) \quad \mathring{\mathbf{V}}_h = \mathcal{P}_1^c(\mathcal{T}_h^{\text{ps}}) \cap \mathbf{H}_0(\text{rot}, \Omega),$$

$$(3.3b) \quad \mathring{Q}_h = \{v \in \mathcal{P}_0(\mathcal{T}_h^{\text{ps}}) \cap L_0^2(\Omega) : \theta_z(v) = 0 \forall z \in \mathcal{S}_h^I(\mathcal{T}_h^{\text{ps}})\}.$$

Lemma 3.2 ([29]). *Let $\mathring{\mathbf{V}}_h$ and \mathring{Q}_h be defined by (3.3). Then there holds $\text{rot } \mathring{\mathbf{V}}_h \subset \mathring{Q}_h$.*

We now extend the results of [29] to construct an appropriate Fortin operator that is well defined for $\tau \in \mathring{\mathbf{V}}(Q_h)$. To do so, we require some additional notation.

For an interior singular vertex $z \in \mathcal{S}_h(\mathcal{T}_h^{\text{ps}})$, let $T \in \mathcal{T}_h$ be a triangle in \mathcal{T}_h such that $z \in \partial T$, and let $\{K_1, K_2\} \subset \mathcal{T}_h^{\text{ps}}$ be the triangles in $\mathcal{T}_h^{\text{ps}}$ such that $K_1, K_2 \subset T$ and $K_1, K_2 \in \mathcal{T}_h^{\text{ps}}(z)$. Let $e = \partial K_1 \cap \partial K_2$, and let \mathbf{m}_i be the outward unit normal of K_i perpendicular to e . We then define the jump of a scalar piecewise smooth function at z (restricted to T) as

$$[[v]]_T(z) = v|_{K_1}(z)\mathbf{m}_1 + v|_{K_2}(z)\mathbf{m}_2.$$

Note that $[[v]]_T(z)$ is single-valued for all $v \in \mathring{Q}_h$. In particular, if z is an interior singular vertex with $z \in \partial T_1 \cap \partial T_2$ for some $T_1, T_2 \in \mathcal{T}_h$, $T_1 \neq T_2$, then $[[v]]_{T_1}(z) = [[v]]_{T_2}(z)$ for all $v \in \mathring{Q}_h$ because $\theta_z(v) = 0$. Therefore, we shall omit the subscript and simply write $[[v]](z)$.

Next for a triangle $T \in \mathcal{T}_h$ in the non-refined mesh, we denote by T^{ct} the resulting set of three triangles obtained by connecting the barycenter of T to its vertices, i.e., T^{ct} is the Clough–Tocher refinement of T . We define the set of (local) piecewise polynomials with respect to this partition as

$$(3.4) \quad \mathcal{P}_k(T^{\text{ct}}) = \prod_{K \in T^{\text{ct}}} \mathcal{P}_k(K).$$

The following lemma provides the degrees of freedom for $\mathring{\mathbf{V}}_h$ and $\mathring{\mathbf{Q}}_h$ that will be used to construct the Fortin operator. The result essentially follows from [29, Lemmas 10–11].

Lemma 3.3. *A function $\boldsymbol{\tau} \in \mathring{\mathbf{V}}_h$ is uniquely defined by the conditions*

$$\begin{aligned}
(3.5a) \quad & \boldsymbol{\tau}(z) && \forall z \in \mathcal{V}_h^I, \\
(3.5b) \quad & \boldsymbol{\tau}(z) \cdot \mathbf{n} && \forall z \in \mathcal{V}_h^B \setminus \mathcal{V}_h^C, \\
(3.5c) \quad & \int_e (\boldsymbol{\tau} \cdot \mathbf{t}) && \forall e \in \mathcal{E}_h^I, \\
(3.5d) \quad & [\mathbf{rot} \boldsymbol{\tau}](z) && \forall z \in \mathcal{S}_h(\mathcal{T}_h^{\text{ps}}), \\
(3.5e) \quad & \int_T (\mathbf{rot} \boldsymbol{\tau})r && \forall r \in \mathcal{P}_0(T^{\text{ct}}) \cap L_0^2(T), \forall T \in \mathcal{T}_h.
\end{aligned}$$

Moreover, a function $v \in \mathring{\mathbf{Q}}_h$ is uniquely determined by the values

$$\begin{aligned}
(3.6a) \quad & [v](z) && \forall z \in \mathcal{S}_h(\mathcal{T}_h^{\text{ps}}), \\
(3.6b) \quad & \int_T vr && \forall r \in \mathring{\mathcal{P}}_0(T^{\text{ct}}), \forall T \in \mathcal{T}_h.
\end{aligned}$$

Theorem 3.4. *Let $\mathring{\mathbf{V}}_h$ and $\mathring{\mathbf{Q}}_h$ be defined by (3.3), and let $\mathring{\mathbf{V}}(Q_h)$ be defined by (2.4). Then there exists a projection $\mathbf{\Pi}_V : \mathring{\mathbf{V}}(Q_h) \rightarrow \mathring{\mathbf{V}}_h$ such that $\mathbf{rot} \mathbf{\Pi}_V \mathbf{p} = \mathbf{rot} \mathbf{p}$ for all $\mathbf{p} \in \mathring{\mathbf{V}}(Q_h)$. Moreover,*

$$\|\boldsymbol{\tau} - \mathbf{\Pi}_V \boldsymbol{\tau}\|_{L^2(\Omega)} \leq C(h^{\frac{1}{2}+\delta} \|\boldsymbol{\tau}\|_{H^{\frac{1}{2}+\delta}(\Omega)} + h \|\mathbf{rot} \boldsymbol{\tau}\|_{L^2(\Omega)}).$$

Proof. Fix $\boldsymbol{\tau} \in \mathring{\mathbf{V}}(Q_h)$, and let $\mathbf{I}_h \boldsymbol{\tau} \in \mathcal{P}_1^c(\mathcal{T}_h) \cap \mathbf{H}_0(\mathbf{rot}, \Omega) \subset \mathring{\mathbf{V}}_h$ be the modified Scott–Zhang interpolant of $\boldsymbol{\tau}$ established in Lemma 3.1. We then construct $\mathbf{\Pi}_V \boldsymbol{\tau}$ via the conditions

$$\begin{aligned}
(3.7a) \quad & (\mathbf{\Pi}_V \boldsymbol{\tau})(z) = (\mathbf{I}_h \boldsymbol{\tau})(z) && \forall z \in \mathcal{V}_h^I, \\
(3.7b) \quad & (\mathbf{\Pi}_V \boldsymbol{\tau})(z) \cdot \mathbf{n} = (\mathbf{I}_h \boldsymbol{\tau})(z) \cdot \mathbf{n} && \forall z \in \mathcal{V}_h^B \setminus \mathcal{V}_h^C, \\
(3.7c) \quad & \int_e (\mathbf{\Pi}_V \boldsymbol{\tau}) \cdot \mathbf{t} = \int_e \boldsymbol{\tau} \cdot \mathbf{t} && \forall e \in \mathcal{E}_h^I, \\
(3.7d) \quad & [\mathbf{rot} \mathbf{\Pi}_V \boldsymbol{\tau}](z) = [\mathbf{rot} \boldsymbol{\tau}](z) && \forall z \in \mathcal{S}_h(\mathcal{T}_h^{\text{ps}}), \\
(3.7e) \quad & \int_T (\mathbf{rot} \mathbf{\Pi}_V \boldsymbol{\tau})r = \int_T (\mathbf{rot} \boldsymbol{\tau})r && \forall r \in \mathcal{P}_0(T^{\text{ct}}) \cap L_0^2(T), \forall T \in \mathcal{T}_h.
\end{aligned}$$

The arguments given in [29] show that $\mathbf{rot} \mathbf{\Pi}_V \boldsymbol{\tau} = \mathbf{rot} \boldsymbol{\tau}$,

By scaling, there holds for each $\boldsymbol{\sigma}_h \in \mathring{\mathbf{V}}_h$ and on each $T \in \mathcal{T}_h$,

$$\begin{aligned}
\|\boldsymbol{\sigma}_h\|_{L^2(T)}^2 &\leq C \left[h_T^2 \left(\sum_{z \in \mathcal{V}_h^I(T)} |\boldsymbol{\sigma}_h(z)|^2 + \sum_{z \in \mathcal{V}_h^B(T) \setminus \mathcal{V}_h^C(T)} |\boldsymbol{\sigma}_h(z) \cdot \mathbf{n}|^2 \right) \right. \\
&\quad + \sum_{e \in \mathcal{E}_h^I(T)} \left| \int_e \boldsymbol{\sigma}_h \cdot \mathbf{t} \right|^2 + h_T^2 \sup_{\substack{r \in \mathcal{P}_0(T^{\text{ct}}) \\ \|r\|_{L^2(T)}=1}} \left| \int_T (\mathbf{rot} \boldsymbol{\sigma}_h)r \right|^2 \\
&\quad \left. + h_T^4 \sum_{z \in \mathcal{S}_h(T)} |[\mathbf{rot} \boldsymbol{\sigma}_h](z)|^2 \right],
\end{aligned}$$

where $\mathcal{S}_h(T)$ is set of singular vertices contained in \bar{T} . Now set $\boldsymbol{\sigma}_h = \mathbf{\Pi}_V \boldsymbol{\tau} - \mathbf{I}_h \boldsymbol{\tau}$. Using the above estimate and (3.7) then yields

$$(3.8) \quad \|\mathbf{\Pi}_V \boldsymbol{\tau} - \mathbf{I}_h \boldsymbol{\tau}\|_{L^2(T)}^2 \leq C \left[\left| \int_{\partial T} (\boldsymbol{\tau} - \mathbf{I}_h \boldsymbol{\tau}) \cdot \mathbf{t} \right|^2 + h_T^2 \sup_{\substack{r \in \mathcal{P}_0(T^{\text{ct}}) \\ \|r\|_{L^2(T)}=1}} \left| \int_T (\text{rot}(\boldsymbol{\tau} - \mathbf{I}_h \boldsymbol{\tau})) r \right|^2 \right. \\ \left. + h_T^4 \sum_{z \in \mathcal{S}_h(T)} |[\text{rot}(\boldsymbol{\tau} - \mathbf{I}_h \boldsymbol{\tau})](z)|^2 \right].$$

Because $\text{rot}(\boldsymbol{\tau} - \mathbf{I}_h \boldsymbol{\tau}) \in \mathring{Q}_h$, we use the degrees of freedom (3.6) and a scaling argument to conclude that

$$(3.9) \quad \sup_{\substack{r \in \mathcal{P}_0(T^{\text{ct}}) \\ \|r\|_{L^2(T)}=1}} \left| \int_T (\text{rot}(\boldsymbol{\tau} - \mathbf{I}_h \boldsymbol{\tau})) r \right|^2 + h_T^2 \sum_{z \in \mathcal{S}_h(T)} |[\text{rot}(\boldsymbol{\tau} - \mathbf{I}_h \boldsymbol{\tau})](z)|^2 \\ \leq C \|\text{rot}(\boldsymbol{\tau} - \mathbf{I}_h \boldsymbol{\tau})\|_{L^2(T)}^2.$$

We then use an inverse estimate to get

$$(3.10) \quad \|\text{rot}(\boldsymbol{\tau} - \mathbf{I}_h \boldsymbol{\tau})\|_{L^2(T)}^2 \leq C [\|\text{rot} \boldsymbol{\tau}\|_{L^2(T)}^2 + \|\nabla \mathbf{I}_h \boldsymbol{\tau}\|_{L^2(T)}] \\ \leq C [\|\text{rot} \boldsymbol{\tau}\|_{L^2(T)}^2 + h_T^{-1+2\delta} \|\mathbf{I}_h \boldsymbol{\tau}\|_{H^{\frac{1}{2}+\delta}(T)}^2].$$

Applying the estimates (3.9)–(3.10) to (3.8), we obtain

$$\|\mathbf{\Pi}_V \boldsymbol{\tau} - \mathbf{I}_h \boldsymbol{\tau}\|_{L^2(T)}^2 \leq C \left[\left| \int_{\partial T} (\boldsymbol{\tau} - \mathbf{I}_h \boldsymbol{\tau}) \cdot \mathbf{t} \right|^2 + h_T^2 (\|\text{rot} \boldsymbol{\tau}\|_{L^2(T)}^2 + h_T^{-1+2\delta} \|\mathbf{I}_h \boldsymbol{\tau}\|_{H^{\frac{1}{2}+\delta}(\omega(T))}^2) \right] \\ \leq C [h_T \|\boldsymbol{\tau} - \mathbf{I}_h \boldsymbol{\tau}\|_{L^2(\partial T)}^2 + h_T^{1+2\delta} \|\mathbf{I}_h \boldsymbol{\tau}\|_{H^{\frac{1}{2}+\delta}(T)}^2 + h_T^2 \|\text{rot} \boldsymbol{\tau}\|_{L^2(T)}^2].$$

We then apply (3.1) and sum over $T \in \mathcal{T}_h$ to obtain

$$\|\mathbf{\Pi}_V \boldsymbol{\tau} - \mathbf{I}_h \boldsymbol{\tau}\|_{L^2(\Omega)} \leq C [h^{\frac{1}{2}+\delta} \|\boldsymbol{\tau}\|_{H^{\frac{1}{2}+\delta}(\Omega)} + h \|\text{rot} \boldsymbol{\tau}\|_{L^2(\Omega)}].$$

Therefore

$$\|\boldsymbol{\tau} - \mathbf{\Pi}_V \boldsymbol{\tau}\|_{L^2(\Omega)} \leq \|\boldsymbol{\tau} - \mathbf{I}_h \boldsymbol{\tau}\|_{L^2(\Omega)} + \|\mathbf{\Pi}_V \boldsymbol{\tau} - \mathbf{I}_h \boldsymbol{\tau}\|_{L^2(\Omega)} \\ \leq C [h^{\frac{1}{2}+\delta} \|\boldsymbol{\tau}\|_{H^{\frac{1}{2}+\delta}(\Omega)} + h \|\text{rot} \boldsymbol{\tau}\|_{L^2(\Omega)}].$$

□

3.2. Construction of Fortin Operator on Clough–Tocher Splits. The Clough–Tocher refinement of \mathcal{T}_h is obtained by connecting the barycenter of each $T \in \mathcal{T}_h$ with its vertices; thus, each triangle is split into three triangles. In this section, we show that there exists a Fortin projection mapping onto the Lagrange finite element space satisfying Assumption 2.3. This result holds for all polynomial degrees $k \geq 2$ but, for simplicity, we only consider the lowest order case $k = 2$.

Let $\mathcal{T}_h^{\text{ct}}$ be the resulting Clough–Tocher refinement of \mathcal{T}_h , and define the spaces

$$(3.11a) \quad \mathring{\mathbf{V}}_h = \mathcal{P}_2^c(\mathcal{T}_h^{\text{ct}}) \cap \mathbf{H}_0(\text{rot}, \Omega),$$

$$(3.11b) \quad \mathring{Q}_h = L_0^2(\Omega) \cap \mathcal{P}_1(\mathcal{T}_h^{\text{ct}}).$$

It is well-known that $\text{rot} \mathring{\mathbf{V}}_h \subset \mathring{Q}_h$ [28].

Below we modify the results in [28] to build a Fortin projection that is well-defined on $\mathbf{H}^{\frac{1}{2}+\delta}(\Omega)$ and has optimal order convergence properties in $\mathbf{L}^2(\Omega)$. To this end, we first provide a useful set of degrees of freedom for $\mathring{\mathbf{V}}_h$ [28].

Lemma 3.5. *A function $\boldsymbol{\tau} \in \mathring{\mathbf{V}}_h$ is uniquely determined by the values*

$$(3.12) \quad \boldsymbol{\tau}(z) \quad \forall z \in \mathcal{V}_h^I,$$

$$(3.13) \quad \boldsymbol{\tau}(z) \cdot \mathbf{n} \quad \forall z \in \mathcal{V}_h^B \setminus \mathcal{V}_h^C,$$

$$(3.14) \quad \int_e \boldsymbol{\tau} \quad \forall e \in \mathcal{E}_h^I,$$

$$(3.15) \quad \int_e \boldsymbol{\tau} \cdot \mathbf{n} \quad \forall e \in \mathcal{E}_h^B,$$

$$(3.16) \quad \int_T (\text{rot } \boldsymbol{\tau}) r \quad \forall r \in \mathcal{P}_1(T^{\text{ct}}) \cap L_0^2(T), \quad \forall T \in \mathcal{T}_h,$$

where $\mathcal{P}_1(T^{\text{ct}})$ is defined by (3.4).

Theorem 3.6. *Let $\mathring{\mathbf{V}}_h$ and $\mathring{\mathbf{Q}}_h$ be defined by (3.11), and let Π_Q be the L^2 projection onto $\mathring{\mathbf{Q}}_h$. Then there exists a projection $\mathbf{\Pi}_V : \mathring{\mathbf{V}}(Q_h) \rightarrow \mathring{\mathbf{V}}_h$, such that $\text{rot } \mathbf{\Pi}_V \boldsymbol{\tau} = \Pi_Q(\text{rot } \boldsymbol{\tau})$. Moreover,*

$$\|\boldsymbol{\tau} - \mathbf{\Pi}_V \boldsymbol{\tau}\|_{L^2(\Omega)} \leq C(h^{\frac{1}{2}+\delta} \|\boldsymbol{\tau}\|_{H^{\frac{1}{2}+\delta}(\Omega)} + h \|\text{rot } \boldsymbol{\tau}\|_{L^2(\Omega)}).$$

Proof. Define $\mathbf{\Pi}_V$ uniquely by the conditions

$$(3.17a) \quad (\mathbf{\Pi}_V \boldsymbol{\tau})(z) = (\mathbf{I}_h \boldsymbol{\tau})(z) \quad \forall z \in \mathcal{V}_h^I,$$

$$(3.17b) \quad (\mathbf{\Pi}_V \boldsymbol{\tau})(z) \cdot \mathbf{n} = (\mathbf{I}_h \boldsymbol{\tau})(z) \cdot \mathbf{n} \quad \forall z \in \mathcal{V}_h^B \setminus \mathcal{V}_h^C,$$

$$(3.17c) \quad \int_e (\mathbf{\Pi}_V \boldsymbol{\tau}) = \int_e \boldsymbol{\tau} \quad \forall e \in \mathcal{E}_h^I,$$

$$(3.17d) \quad \int_e (\mathbf{\Pi}_V \boldsymbol{\tau} \cdot \mathbf{n}) = \int_e \boldsymbol{\tau} \cdot \mathbf{n} \quad \forall e \in \mathcal{E}_h^B,$$

$$(3.17e) \quad \int_T (\text{rot } \mathbf{\Pi}_V \boldsymbol{\tau}) r = \int_T (\text{rot } \boldsymbol{\tau}) r \quad \forall r \in \mathcal{P}_1(T^{\text{ct}}) \cap L_0^2(T), \quad \forall T \in \mathcal{T}_h.$$

The arguments given in [28] show that $\text{rot } \mathbf{\Pi}_V \boldsymbol{\tau} = \Pi_Q \text{rot } \boldsymbol{\tau}$. The same scaling arguments given in Theorem 3.4 show that $\|\boldsymbol{\tau} - \mathbf{\Pi}_V \boldsymbol{\tau}\|_{L^2(\Omega)} \leq C(h^{\frac{1}{2}+\delta} \|\boldsymbol{\tau}\|_{H^{\frac{1}{2}+\delta}(\Omega)} + h \|\text{rot } \boldsymbol{\tau}\|_{L^2(\Omega)})$. \square

3.3. Construction of Fortin Operator on General Triangulations. In this section, we construct a Fortin operator for the original Scott–Vogelius pair developed in [40]. This pair essentially takes the space $\mathring{\mathbf{V}}_h$ to be the Lagrange space of degree $k \geq 4$, and $\mathring{\mathbf{Q}}_h$ to be the space of piecewise polynomials of degree $(k-1)$. As pointed out in [40] the exact definition of these spaces and their stability is mesh-dependent and depends on the presence of singular or “nearly singular” vertices.

Recall that a singular vertex is a vertex in \mathcal{T}_h that lies on exactly two straight lines. To make this precise, for a vertex $z \in \mathcal{V}_h$, we enumerate the triangles that have z as a vertex as $\mathcal{T}_h(z) = \{T_1, T_2, \dots, T_N\}$. If z is a boundary vertex then we enumerate the triangles such that T_1 and T_N have a boundary edge. Moreover, we enumerate them so that T_j, T_{j+1} share an edge for $j = 1, \dots, N-1$ and T_N and T_1 share an edge in the case z is an interior vertex. Let θ_j denote the angle between the edges of T_j originating from z . We define

$$(3.18) \quad \Theta(z) = \begin{cases} \max\{|\sin(\theta_1 + \theta_2)|, \dots, |\sin(\theta_{N-1} + \theta_N)|, |\sin(\theta_N + \theta_1)|\} & \text{if } z \in \mathcal{V}_h^I \\ \max\{|\sin(\theta_1 + \theta_2)|, \dots, |\sin(\theta_{N-1} + \theta_N)|\} & \text{if } z \in \mathcal{V}_h^B \text{ and } N \geq 2, \\ 0 & \text{if } z \in \mathcal{V}_h^B \text{ and } N = 1. \end{cases}$$

Definition 3.7. A vertex $z \in \mathcal{V}_h$ is a singular vertex if $\Theta(z) = 0$. It is non-singular if $\Theta(z) > 0$.

We denote all the singular vertices by

$$\mathcal{S}_h = \{z \in \mathcal{V}_h : \Theta(z) = 0\}.$$

We further let \mathcal{S}_h^I denote the set of interior singular vertices, \mathcal{S}_h^B the set of boundary singular vertices, and \mathcal{S}_h^C the set of corner singular vertices. Equivalently,

$$\begin{aligned}\mathcal{S}_h^I &= \{z \in \mathcal{S}_h : \#\mathcal{T}_h(z) = 4\}, \\ \mathcal{S}_h^B &= \{z \in \mathcal{S}_h : \#\mathcal{T}_h(z) \in \{1, 2\}\}, \\ \mathcal{S}_h^C &= \{z \in \mathcal{S}_h : \#\mathcal{T}_h(z) = 1\}.\end{aligned}$$

Definition 3.8. We set

$$(3.19) \quad \Theta_{\min} := \min_{z \in \mathcal{V}_h \setminus \mathcal{S}_h} \Theta(z).$$

For a non-negative integer k , we define the spaces

$$(3.20a) \quad \mathring{\mathbf{V}}_h = \mathcal{P}_k^c(\mathcal{T}_h) \cap \mathbf{H}_0(\text{rot}, \Omega),$$

$$(3.20b) \quad \mathring{\mathbf{Q}}_h = \{v \in L_0^2(\Omega) \cap \mathcal{P}_{k-1}(\mathcal{T}_h) : \theta_z(v) = 0 \ \forall z \in \mathcal{S}_h^I, \ v(z) = 0 \ \forall z \in \mathcal{S}_h^C\},$$

where we recall that $\theta_z(v)$ is defined by (3.2).

First we note that the rot operator maps $\mathring{\mathbf{V}}_h$ into $\mathring{\mathbf{Q}}_h$ [40].

Lemma 3.9. *There holds $\text{rot } \boldsymbol{\tau} \in \mathring{\mathbf{Q}}_h$ for all $\boldsymbol{\tau} \in \mathring{\mathbf{V}}_h$.*

Let \mathbf{I}_h be Scott-Zhang interpolant onto $\mathcal{P}_1^c(\mathcal{T}_h) \cap \mathbf{H}_0(\text{rot}; \Omega) \subset \mathring{\mathbf{V}}_h$. Then define $\mathbf{I}_1 : \mathbf{H}^{\frac{1}{2}+\delta}(\Omega) \rightarrow \mathring{\mathbf{V}}_h$ as follows

$$\begin{aligned}\mathbf{I}_1 \boldsymbol{\tau}(z) &= \mathbf{I}_h \boldsymbol{\tau}(z) \quad \forall z \in \mathcal{V}_h, \\ \int_e \mathbf{I}_1 \boldsymbol{\tau} \cdot \boldsymbol{\psi} &= \int_e \boldsymbol{\tau} \cdot \boldsymbol{\psi} \quad \text{for all } \boldsymbol{\psi} \in \mathcal{P}_{k-2}(e), \ \forall e \in \mathcal{E}_h, \\ \int_T \mathbf{I}_1 \boldsymbol{\tau} \cdot \boldsymbol{\psi} &= \int_T \boldsymbol{\tau} \cdot \boldsymbol{\psi} \quad \text{for all } \boldsymbol{\psi} \in \mathcal{P}_{k-3}(T), \ \forall T \in \mathcal{T}_h.\end{aligned}$$

Standard arguments yield the following result.

Lemma 3.10. *There holds for all $\boldsymbol{\tau} \in \mathbf{H}^{\frac{1}{2}+\delta}(\Omega)$*

$$(3.21) \quad \|\boldsymbol{\tau} - \mathbf{I}_1 \boldsymbol{\tau}\|_{L^2(\Omega)} \leq Ch^{\frac{1}{2}+\delta} \|\boldsymbol{\tau}\|_{\mathbf{H}^{\frac{1}{2}+\delta}(\Omega)},$$

and

$$(3.22) \quad \|\text{rot}(\mathbf{I}_1 \boldsymbol{\tau})\|_{L^2(\Omega)} \leq h^{-\frac{1}{2}+\delta} \|\boldsymbol{\tau}\|_{\mathbf{H}^{\frac{1}{2}+\delta}(\Omega)}.$$

Moreover, for $k \geq 2$,

$$(3.23) \quad \int_T \text{rot } \mathbf{I}_1 \boldsymbol{\tau} = \int_T \text{rot } \boldsymbol{\tau} \quad \forall T \in \mathcal{T}_h.$$

The following result follows from [31, Lemma 6].

Lemma 3.11. *Suppose that $k \geq 4$. Then there exists an injective linear operator $\mathbf{J}_1 : \mathring{\mathbf{Q}}_h \rightarrow \mathring{\mathbf{V}}_h$ such that*

$$(3.24a) \quad \text{rot}(\mathbf{J}_1 v)(z) = v(z) \quad \forall z \in \mathcal{V}_h,$$

$$(3.24b) \quad \int_T \text{rot}(\mathbf{J}_1 v) \, dx = 0 \quad \forall T \in \mathcal{T}_h,$$

$$(3.24c) \quad \|\mathbf{J}_1 v\|_{L^2(\Omega)} + h \|\nabla \mathbf{J}_1 v\|_{L^2(\Omega)} \leq Ch \left(\frac{1}{\Theta_{\min}} + 1 \right) \|v\|_{L^2(\Omega)}.$$

The following result follows from [40, 27, 31].

Lemma 3.12. *Define*

$$\mathring{Q}_h = \{v \in \mathring{Q}_h : \int_T v = 0 \ \forall T \in \mathcal{T}_h, \text{ and } v(z) = 0 \ \forall z \in \mathcal{V}_h\}.$$

Then there exists an injective operator $\mathbf{J}_2 : \mathring{Q}_h \rightarrow \mathring{V}_h$ such that

$$\begin{aligned} \text{rot}(\mathbf{J}_2 v) &= v, \\ \|\mathbf{J}_2 v\|_{L^2(\Omega)} + h \|\nabla \mathbf{J}_2 v\|_{L^2(\Omega)} &\leq Ch \|v\|_{L^2(\Omega)}. \end{aligned}$$

Theorem 3.13. *Let \mathring{V}_h and \mathring{Q}_h be defined by (3.20) with $k \geq 4$. Then there exists a projection $\mathbf{\Pi}_V : \mathring{V}(Q_h) \rightarrow \mathring{V}_h$ such that*

$$\text{rot}(\mathbf{\Pi}_V \boldsymbol{\tau}) = \text{rot } \boldsymbol{\tau}$$

with the following bound

$$\|\boldsymbol{\tau} - \mathbf{\Pi}_V \boldsymbol{\tau}\|_{L^2(\Omega)} \leq C(1 + \Theta_{\min}^{-1}) h^{\frac{1}{2} + \delta} \|\boldsymbol{\tau}\|_{H^{\frac{1}{2} + \delta}(\Omega)}.$$

Proof. Define:

$$\mathbf{\Pi}_V \boldsymbol{\tau} = \mathbf{I}_1 \boldsymbol{\tau} + \mathbf{J}_1 v_1 + \mathbf{J}_2 v_2 \in \mathring{V}_h,$$

where

$$v_1 = \text{rot}(\boldsymbol{\tau} - \mathbf{I}_1 \boldsymbol{\tau}) \in \mathring{Q}_h, \quad v_2 = v_1 - \text{rot}(\mathbf{J}_1 v_1) \in \mathring{Q}_h.$$

By Lemma 3.11 and the definition of v_2 , we see that

$$v_2(z) = 0 \quad \forall z \in \mathcal{V}_h,$$

and

$$\int_T v_2 = \int_T (v_1 - \text{rot}(\mathbf{J}_1 v_1)) = \int_T v_1 = \int_T \text{rot}(\boldsymbol{\tau} - \mathbf{I}_1 \boldsymbol{\tau}) = 0,$$

by Lemma 3.10. Therefore $v_2 \in \mathring{Q}_h$, and so $\mathbf{J}_2 v_2$ is well-defined (cf. Lemma 3.12).

We then use Lemma 3.12 to get

$$\begin{aligned} \text{rot}(\mathbf{\Pi}_V \boldsymbol{\tau}) &= \text{rot}(\mathbf{I}_1 \boldsymbol{\tau}) + \text{rot}(\mathbf{J}_1 v_1) + \text{rot}(\mathbf{J}_2 v_2) \\ &= \text{rot}(\mathbf{I}_1 \boldsymbol{\tau}) + \text{rot}(\mathbf{J}_1 v_1) + v_2 \\ &= \text{rot}(\mathbf{I}_1 \boldsymbol{\tau}) + \text{rot}(\mathbf{J}_1 v_1) + (v_1 - \text{rot}(\mathbf{J}_1 v_1)) \\ &= \text{rot}(\mathbf{I}_1 \boldsymbol{\tau}) + v_1 \\ &= \text{rot}(\mathbf{I}_1 \boldsymbol{\tau}) + \text{rot}(\boldsymbol{\tau} - \mathbf{I}_1 \boldsymbol{\tau}) \\ &= \text{rot } \boldsymbol{\tau}. \end{aligned}$$

Now we note that, by (3.22),

$$\begin{aligned} \|\text{rot}(\boldsymbol{\tau} - \mathbf{I}_1 \boldsymbol{\tau})\|_{L^2(\Omega)} &\leq \|\text{rot } \boldsymbol{\tau}\|_{L^2(\Omega)} + \|\text{rot}(\mathbf{I}_1 \boldsymbol{\tau})\|_{L^2(\Omega)} \\ (3.25) \quad &\leq \|\text{rot } \boldsymbol{\tau}\|_{L^2(\Omega)} + h^{-\frac{1}{2} + \delta} \|\boldsymbol{\tau}\|_{H^{\frac{1}{2} + \delta}(\Omega)}. \end{aligned}$$

Next, by Lemma 3.11 and (3.25) we obtain

$$\begin{aligned} (3.26) \quad \|\mathbf{J}_1 v_1\|_{L^2(\Omega)} &\leq Ch \left(\frac{1}{\Theta_{\min}} + 1 \right) \|v_1\|_{L^2(\Omega)} \\ &\leq Ch \left(\frac{1}{\Theta_{\min}} + 1 \right) \|\text{rot}(\boldsymbol{\tau} - \mathbf{I}_1 \boldsymbol{\tau})\|_{L^2(\Omega)} \\ &\leq C \left(\frac{1}{\Theta_{\min}} + 1 \right) (h \|\text{rot } \boldsymbol{\tau}\|_{L^2(\Omega)} + h^{\frac{1}{2} + \delta} \|\boldsymbol{\tau}\|_{H^{\frac{1}{2} + \delta}(\Omega)}). \end{aligned}$$

Likewise, we use Lemmas 3.12 and (3.25) to obtain

$$\begin{aligned}
(3.27) \quad \|\mathbf{J}_2 v_2\|_{L^2(\Omega)} &\leq Ch\|v_2\|_{L^2(\Omega)} \\
&\leq Ch(\|v_1\|_{L^2(\Omega)} + \|\text{rot}(\mathbf{J}_1 v_1)\|_{L^2(\Omega)}) \\
&\leq C(h\|\text{rot}(\boldsymbol{\tau} - \mathbf{I}_1 \boldsymbol{\tau})\|_{L^2(\Omega)} + \|\mathbf{J}_1 v_1\|_{L^2(\Omega)}) \\
&\leq C\left(\frac{1}{\Theta_{\min}} + 1\right)(h\|\text{rot} \boldsymbol{\tau}\|_{L^2(\Omega)} + h^{\frac{1}{2}+\delta}\|\boldsymbol{\tau}\|_{H^{\frac{1}{2}+\delta}(\Omega)}).
\end{aligned}$$

We then use the triangle inequality, Lemma 3.10, (3.26), and (3.27) to obtain the L^2 error estimate:

$$\begin{aligned}
\|\boldsymbol{\tau} - \boldsymbol{\Pi}_V \boldsymbol{\tau}\|_{L^2(\Omega)} &\leq \|\boldsymbol{\tau} - \mathbf{I}_1 \boldsymbol{\tau}\|_{L^2(\Omega)} + \|\mathbf{J}_1 v_1\|_{L^2(\Omega)} + \|\mathbf{J}_2 v_2\|_{L^2(\Omega)} \\
&\leq C\left(\frac{1}{\Theta_{\min}} + 1\right)h^{\frac{1}{2}+\delta}\|\boldsymbol{\tau}\|_{H^{\frac{1}{2}+\delta}(\Omega)}.
\end{aligned}$$

Finally, if $\boldsymbol{\tau} \in \mathring{\mathbf{V}}_h$, then $\mathbf{I}_1 \boldsymbol{\tau} = \boldsymbol{\tau}$ and so $v_1 = 0$. It then follows that $\mathbf{J}_1 v_1 = 0$, and $\mathbf{J}_2 v_2 = -\mathbf{J}_2(\text{rot}(\mathbf{J}_1 v_1)) = 0$. Therefore $\boldsymbol{\Pi}_V \boldsymbol{\tau} = \mathbf{I}_1 \boldsymbol{\tau} = \boldsymbol{\tau}$, i.e., $\boldsymbol{\Pi}_V$ is a projection. \square

4. NUMERICAL EXPERIMENTS

In this section we confirm the theoretical results with some numerical experiments on a variety of meshes and finite element spaces. All the numerical experiments were performed using FEniCS [1]. In the first four tests, we take the domain to be the unit square $\Omega = (0, 1)^2$. The exact eigenvectors, corresponding to non-zero eigenvalues, are $\mathbf{u}^{(n,m)}(x, y) := \mathbf{curl} p^{(n,m)}$ where $p^{(n,m)} := \cos(\pi n x) \cos(\pi m y)$, with eigenvalues $\lambda^{(n,m)} := \pi^2(n^2 + m^2)$ for $n, m \in \mathbb{N} \cup \{0\}$ and $nm \neq 0$. In the following we relabel the non-zero eigenvalues $\lambda^{(i)}$ in non-decreasing order: $0 < \lambda^{(1)} \leq \lambda^{(2)} \leq \lambda^{(3)} \leq \dots$

4.1. Linear Lagrange elements on Powell–Sabin triangulations. In these series of tests, we compute the finite element method (1.2) using piecewise linear Lagrange elements defined on Powell–Sabin triangulations. We create a sequence of generic Delaunay triangulations \mathcal{T}_h with mesh size $h_j = 2^{-j}$ for $j = 3, 4, 5, 6$, and perform the refinement algorithm described in Section 3.1 to obtain a Powell–Sabin triangulation $\mathcal{T}_h^{\text{PS}}$ for each mesh parameter.

In Table 1, we show the first ten non-zero approximate eigenvalues and errors using method (1.2) defined on $\mathcal{T}_h^{\text{PS}}$ for fixed $h = 1/32$. In Table 2, we list the rate of convergence of the first eigenvalue with respect to h . The tables show an absence of spurious eigenvalues which agrees with the theoretical results, Theorems 2.4 and 3.4. In addition, we observe an asymptotic quadratic rate of convergence for the computed eigenvalue.

i	$\lambda_h^{(i)}$	$ \lambda^{(i)} - \lambda_h^{(i)} $
1	9.872556542826	2.952141736802360E-3
2	9.872647617226	3.043216136799032E-3
3	19.75126057536	1.205177318315975E-2
4	39.52514303832	4.672543396706175E-2
5	39.52979992791	5.138232355238159E-2
6	49.42354393173	7.552192628650545E-2
7	49.43033089264	8.230888719544538E-2
8	79.15457141878	1.977362100693938E-1
9	89.06160447391	2.351648641029839E-1
10	89.07453060702	2.480909972125715E-1

TABLE 1. Approximate eigenvalues of (1.2) using the piecewise linear Lagrange finite element space on a Powell–Sabin triangulation. The mesh parameter is $h = 2^{-5}$.

h	$ \lambda^{(1)} - \lambda_h^{(1)} $	rate
2^{-3}	1.084194558097806E-1	
2^{-4}	3.835460507298371E-2	1.8228
2^{-5}	2.952141736802360E-3	1.8768
2^{-6}	7.488421347368046E-4	1.9790

TABLE 2. The rate of convergence with respect to h of first non-zero eigenvalue using for Powell–Sabin split and the linear Lagrange finite element space.

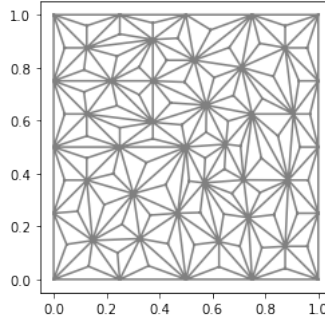


FIGURE 2. A Clough–Tocher triangulation with $h = 2^{-3}$.

4.2. Quadratic Lagrange elements on Clough–Tocher triangulations. In this section, we compute the finite element method (1.2) using quadratic Lagrange elements defined on Clough–Tocher triangulations (cf. Section 3.2). As before, we create a sequence of meshes \mathcal{T}_h with $h_j = 2^{-j}$ ($j = 3, 4, 5, 6$), and construct the Clough–Tocher refinement $\mathcal{T}_h^{\text{ct}}$ by connecting the vertices of each triangle in \mathcal{T}_h with its barycenter; see Figure 4.2.

In Table 3 we report the first computed ten non-zero approximate eigenvalues using method (1.2). As predicted by Theorems 2.4 and 3.6, the results show accurate approximations with no spurious eigenvalues. In Table 4 we list the rate of convergence to the first eigenvalue for different values of h . The table clearly shows an asymptotic quartic rate of convergence: $|\lambda^{(1)} - \lambda_h^{(1)}| = \mathcal{O}(h^4)$.

i	$\lambda_h^{(i)}$	$ \lambda^{(i)} - \lambda_h^{(i)} $
1	9.869606458779	2.057689641788E-6
2	9.869606625899	2.224809986018E-6
3	19.73922733515	1.853298115861E-5
4	39.47853970719	1.221028349079E-4
5	39.47855143244	1.338280896661E-4
6	49.34827341503	2.514095869017E-4
7	49.34829772352	2.757180775106E-4
8	78.95794423573	1.109027018615E-3
9	88.82788915584	1.449546038714E-3
10	88.82798471962	1.545109821734E-3

TABLE 3. Approximate eigenvalues using quadratic Lagrange elements on a Clough–Tocher triangulation with $h = 2^{-5}$.

4.3. Quartic Lagrange elements on criss-cross triangulations. In this section we compute the finite element method (1.2) using fourth degree Lagrange elements on several types of triangulations.

h	$ \lambda^{(1)} - \lambda_h^{(1)} $	rate
2^{-3}	2.98012061403341E-4	
2^{-4}	2.96722579697928E-5	3.3282
2^{-5}	2.05768964178787E-6	3.8500
2^{-6}	1.43249797801559E-7	3.8444

TABLE 4. The rate of convergence of first non-zero eigenvalue using the Clough–Tocher split and $k = 2$

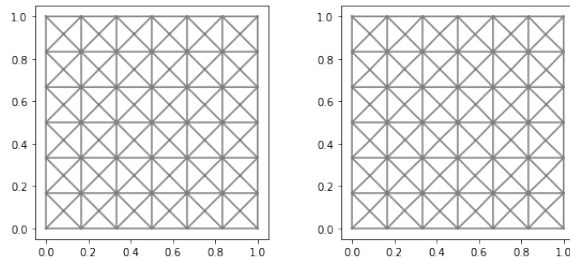


FIGURE 3. Left: Criss-cross mesh with $h = 1/6$. Right: The mesh obtained by randomly perturbing the singular vertices of the criss-cross mesh by $0.01h$.

Theorems 2.4 and 3.13 indicate that this scheme leads to convergent eigenvalue approximations as $h \rightarrow 0$ if the quantity Θ_{\min} is uniformly bounded from below. We recall that the quantity Θ_{\min} gives a measurement of the closest to singular vertex in the mesh, i.e., Θ_{\min} is small if there exists a vertex in \mathcal{T}_h that falls on two “almost” straight lines; see (3.19) and (3.18) for the precise definition.

In the first series of tests, we numerically study the effect of Θ_{\min} in the finite element method (1.2). To this end, we first take \mathcal{T}_h to be the criss-cross mesh with $h = 1/6$ (cf. Figure 4.3). This triangulation has 36 singular vertices, but Θ_{\min} is well-behaved. Theorems 2.4 and 3.13 indicate that the finite element scheme (1.2) (with quartic Lagrange elements) leads to accurate approximations. Indeed, Table 5 lists the first ten computed non-zero eigenvalues, and it clearly shows accurate results.

Next, we perform the same tests but randomly perturb each singular vertex of the criss-cross mesh by a factor αh for some $\alpha \in (0, 1]$. In particular, for each singular vertex $z \in \mathcal{S}_h$ of the criss-cross triangulation \mathcal{T}_h , we make the perturbation $z \rightarrow z + (\pm\alpha h, \pm\alpha h)$. Figures 4.3(right), 4.3(left), and 4.3(right) show the resulting triangulations with $\alpha = 0.01$, $\alpha = 0.05$, and $\alpha = 0.1$, respectively. We note that on the resulting perturbed mesh, $\Theta_{\min} \approx \alpha$, and therefore Theorem 3.13 suggests that the finite element approximation (1.2) may suffer for small α -values.

The computed eigenvalues, with values $\alpha = 0.01$, $\alpha = 0.05$, and $\alpha = 0.1$, are reported in Tables 6, 7, and 8, respectively. Table 8 shows that, for relatively large perturbations ($\alpha = 0.1$), we compute relatively accurate eigenvalue approximations with similar convergence properties found on the criss-cross mesh (cf. Table 5). On the other hand, for smaller perturbations ($\alpha = 0.05$ and $\alpha = 0.01$), the results drastically differ. Table 6 clearly shows extremely poor approximations for all eigenvalues, and Table 7 only computes the first few eigenvalues with reasonable accuracy before the results deteriorate. These numerical tests indicate the approximation properties of the computed eigenvalues are highly sensitive to the quantity Θ_{\min} .

4.4. Quartic Lagrange elements on generic triangulations. Our next series of tests compute the finite element method (1.2) using quartic Lagrange elements on generic Delaunay triangulations. Again, Theorem 3.13 and the previous set of tests indicate the approximation properties of the computed eigenvalues are highly sensitive to the quantity Θ_{\min} . In light of this, for a given (generic)

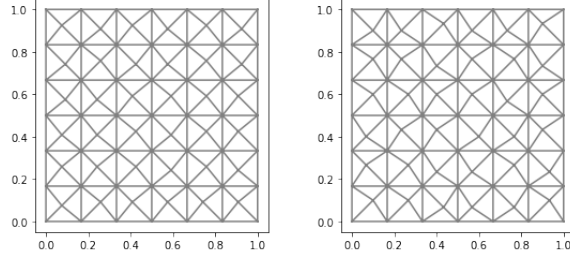


FIGURE 4. Criss-cross meshes with singular vertices randomly perturbed by $0.05h$ (left) and $0.1h$ (right).

i	$\lambda_h^{(i)}$	$ \lambda^{(i)} - \lambda_h^{(i)} $
1	9.869604401309	2.199112003609E-10
2	9.869604401309	2.200408744102E-10
3	19.73920880459	2.414715538634E-09
4	39.47841782951	2.251546860066E-07
5	39.47841782951	2.251547499554E-07
6	49.34802238840	3.829525141441E-07
7	49.34802238840	3.829534165334E-07
8	78.95683762620	2.417486058448E-06
9	88.82645223886	1.262905662713E-05
10	88.82645223886	1.262905958299E-05

TABLE 5. Approximate eigenvalues using quartic Lagrange elements on a criss-cross mesh with $h = 1/6$.

i	$\lambda_h^{(i)}$	$ \lambda^{(i)} - \lambda_h^{(i)} $
1	1.424154538647	8.445449862442
2	1.471404605901	8.398199795188
3	1.477776343297	18.26143245888
4	1.502342236815	37.97607536754
5	1.526468793982	37.95194881038
6	1.540736126805	47.80728587864
7	1.552154885100	47.79586712035
8	1.556952619119	77.39988258960
9	1.566640464185	87.25979914562
10	1.580713040988	87.24572656882

TABLE 6. Approximate eigenvalues using quartic Lagrange elements on a $0.01h$ -perturbed criss-cross mesh with $h = 1/6$.

triangulation \mathcal{T}_h we randomly move each interior vertex with four neighboring triangles by a $0.1h$ -perturbation; see Figure 4.4.

Table 10 shows the maximum errors of the first 20 computed eigenvalues on these perturbed mesh for $h = 2^{-j}$ ($j = 2, 3, 4, 5$). The table clearly shows convergence with rate $\mathcal{O}(h^8)$. On the other hand, the errors of the computed eigenvalues on ‘non-perturbed’ meshes do not converge as shown in Table 9.

i	$\lambda_h^{(i)}$	$ \lambda^{(i)} - \lambda_h^{(i)} $
1	9.869604401311	2.212932059820E-10
2	9.869604401311	2.215134742301E-10
3	19.73920880479	2.614239491550E-09
4	35.63498774612	3.843429858239
5	36.48359498561	2.994822618752
6	36.92351459416	12.42450741128
7	37.63299206644	11.71502993900
8	37.78514981304	41.17168539568
9	38.10084364520	50.72559596460
10	38.35191236801	50.47452724179

TABLE 7. Approximate eigenvalues using quartic Lagrange elements on a $0.05h$ -perturbed criss-cross mesh with $h = 1/6$.

i	$\lambda_h^{(i)}$	$ \lambda^{(i)} - \lambda_h^{(i)} $
1	9.869604401320	2.310134306071E-10
2	9.869604401320	2.312834368468E-10
3	19.73920880546	3.285371974471E-09
4	39.47841784038	2.36019999885E-07
5	39.47841784071	2.363495781310E-07
6	49.34802242662	4.211773898533E-07
7	49.34802246288	4.574410894520E-07
8	78.95683842488	3.216167357323E-06
9	88.82645270371	1.309390694360E-05
10	88.82645276747	1.315766178323E-05

TABLE 8. Approximate eigenvalues using quartic Lagrange elements on a $0.1h$ -perturbed criss-cross mesh with $h = 1/6$.

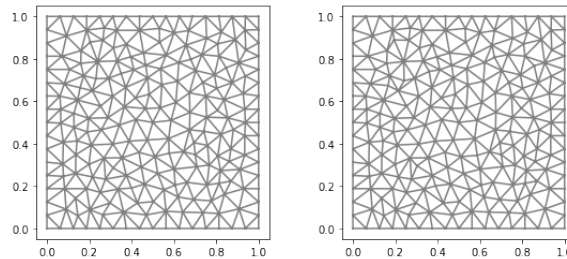


FIGURE 5. (left) Unstructured mesh with $h \approx 1/10$, (right) randomly perturbing interior vertices who have four triangles by at most $.1h$

It is interesting to note that Costabel and Dauge [19] showed that using quartics one has convergence on any mesh if they use they add a (div, div) stabilization term to the formulation (at least for convex polygons). However, here we see that the results are more sensitive with the formulation (1.1).

4.5. L-Shaped Domains. In this example, we consider an L -shaped domain:

$\Omega = [-\pi, \pi]^2 \setminus ([0, \pi] \times [-\pi, 0])$. The first non-zero eigenvalue corresponds to an eigenvector that is not in H^1 and the approximate value of this eigenvalue is given by $\lambda^{(1)} \approx 0.149511749824251$ [20].

h	$\max_{1 \leq i \leq 20} \lambda^{(i)} - \lambda_h^{(i)} $	rate
2^{-2}	8.38611345105E-03	
2^{-3}	5.61831120933E-05	7.2217
2^{-4}	59.2176263988	-20.008
2^{-5}	59.2176264065	0.000

TABLE 9. Maximum error of the first 20 eigenvalues on (non-perturbed) Delaunay triangulations using quartic Lagrange elements. Note that for $h = 2^{-2}$ and $h = 2^{-3}$, the mesh \mathcal{T}_h does not have any vertices with four neighboring triangles.

h	$\max_{1 \leq i \leq 20} \lambda^{(i)} - \lambda_h^{(i)} $	rate
2^{-2}	8.3861134511E-03	
2^{-3}	5.6183112093E-05	7.2217
2^{-4}	2.2360291041E-07	7.9731
2^{-5}	8.9832496997E-10	7.9595

TABLE 10. Maximum error of the first 20 eigenvalues on perturbed Delaunay triangulations using quartic Lagrange elements.

In Table 11 we give the error using Lagrange elements with $k = 1$ on Powell-Sabin splits. In Table 12 we give the error using Nédélec elements of the second kinds with $k = 1$ on the same meshes. As we can see, the rate of convergence seems to be tending to $4/3$ for both finite elements. The next eigenvalues correspond to eigenvectors that belong to H^1 and the convergence rates increase to 2 for both elements, but we do not present the errors here.

We would like to stress that although the eigenvalues do converge as we proved, the convergence of the eigenvectors will not converge in $H(\text{div}) \cap H(\text{curl})$ if the eigenfunctions are not in H^1 . Instead convergence should be sought in the $H(\text{curl})$ norm.

h	$ \lambda^{(1)} - \lambda_h^{(1)} $	rate
2^{-3}	5.29957E-03	
2^{-4}	2.42718E-03	1.12659499
2^{-5}	1.07087E-03	1.18049541
2^{-6}	5.5788E-04	0.94076660
2^{-7}	1.8099E-04	1.62402935
2^{-8}	7.273E-05	1.31537097

TABLE 11. L -shaped domain: The rate of convergence of first non-zero eigenvalue using the Powell-Sabin split and $k = 1$

5. CONCLUDING REMARKS

In this paper, we studied and numerically verified the use of Lagrange finite element spaces for the two-dimensional Maxwell eigenvalue problem. Using and extending the analysis of divergence-free Stokes pairs, we showed, on certain triangulations, convergence of the discrete eigenvalues.

While the focus of this paper has been on the two-dimensional setting, the tools developed here may apply to three dimensions as well. In particular, smooth, discrete de Rham complexes using Lagrange finite element spaces have been constructed in [28, 30], and these results might be applicable to the 3D Maxwell eigenvalue problem.

h	$ \lambda^{(1)} - \lambda_h^{(1)} $	rate
2^{-3}	9.564E-05	
2^{-4}	6.285E-05	0.60567278
2^{-5}	3.039E-05	1.04839118
2^{-6}	1.763E-05	0.78534429
2^{-7}	5.72E-06	1.62460510
2^{-8}	2.41E-06	1.24527844

TABLE 12. L -shaped domain: The rate of convergence of first non-zero eigenvalue using the Nédélec elements of the second kind and $k = 1$

REFERENCES

- [1] M. S. Alnaes, J. Blechta, J. Hake, A. Johansson, B. Kehlet, A. Logg, C. Richardson, J. Ring, M. E. Rognes and G. N. Wells, *The FEniCS Project Version 1.5*, Archive of Numerical Software, vol. 3, 2015.
- [2] C. Amrouche, C. Bernardi, M. Dauge, and V. Girault, *Vector potential in three dimensional nonsmooth domains*, Math. Methods Appl. Sci., 21:823–864, 1998.
- [3] D.N. Arnold, R.S. Falk, and R. Winther, *Finite element exterior calculus: from Hodge theory to numerical stability*, Bull. Amer. Math. Soc. (N.S.), 47(2):281–354, 2010.
- [4] D.N. Arnold, R.S. Falk, and R. Winther, *Finite element exterior calculus, homological techniques, and applications*, Acta Numerica. 2006:1–55.
- [5] I. Babuška and J. Osborn, *Eigenvalue Problems*, in Handbook of Numerical Analysis, II:641–787, North–Holland, Amsterdam, 1991.
- [6] S. Badia and R. Codina, *A nodal-based finite element approximation of the Maxwell problem suitable for singular solutions*, SIAM J. Numer. Anal., 50(2):398–417, 2012.
- [7] J.C. Bellido, C. Mora-Corral, *Existence for nonlocal variational problems in peridynamics*, SIAM Journal on Mathematical Analysis, 46(1):890–916, 2014.
- [8] D. Boffi, *Finite element approximation of eigenvalue problems*, Acta Numer., 1–120, 2010.
- [9] D. Boffi, F. Brezzi, and L. Gastaldi, *On the problem of spurious eigenvalues in the approximation of linear elliptic problems in mixed form*, Math. Comp., 69(229):121–140, 2000.
- [10] D. Boffi, F. Brezzi, L. Demkowicz, R.G. Durán, R.S. Falk, and M. Fortin, *Mixed finite elements, compatibility conditions, and applications*, Lectures given at the C.I.M.E. Summer School held in Cetraro, June 26–July 1, 2006. Edited by Boffi and Lucia Gastaldi. Lecture Notes in Mathematics, 1939. Springer-Verlag, Berlin; Fondazione C.I.M.E., Florence, 2008.
- [11] D. Boffi, P. Fernandes, L. Gastaldi, and I. Perugia, *Computational models of electromagnetic resonators: analysis of edge element approximation*, SIAM J. Numer. Anal., 36(4):1264–1290, 1999.
- [12] A. Bonito and J.-L. Guermond, *Approximation of the eigenvalue problem for the time harmonic Maxwell system by continuous Lagrange finite elements*, Math. Comp., 80(276):1887–1910, 2011.
- [13] A. Buffa, P. Ciarlet Jr., and E. Jamelot, *Solving electromagnetic eigenvalue problems in polyhedral domains with nodal finite elements*, Numer. Math., 113(4):497–518, 2009.
- [14] S.H. Christiansen and K. Hu, *Generalized finite element systems for smooth differential forms and Stokes’ problem*, Numerische Mathematik. 2018 Oct;140(2):327–71.
- [15] S. Christiansen and R. Winther, *Smoothed projections in finite element exterior calculus*, Mathematics of Computation. 2008;77(262):813–29.
- [16] P. Ciarlet, *Analysis of the Scott–Zhang interpolation in the fractional order Sobolev spaces*, J. Num. Math., 21(3):173–180, 2013.
- [17] M. Costabel and M. Dauge, *Maxwell and Lamé eigenvalues on polyhedra*, Math. Meth. Appl. Sci., 22:243–258, 1999.
- [18] M. Costabel, M. Dauge, and S. Nicaise, *Singularities of Maxwell interface problems*, Math. Modell. Numer. Anal., 33:627–649, 1999.
- [19] M. Costabel and M. Dauge, *Weighted regularization of Maxwell equations in polyhedral domains. A rehabilitation of nodal finite elements*, Numer. Math., 93(2):239–277, 2002.
- [20] M. Dauge, *Benchmark computations for Maxwell equations for the approximation of highly singular solutions*, URL: <https://perso.univ-rennes1.fr/monique.dauge/benchmax.html>.
- [21] I. Drelichman and R. G. Durán, *Improved Poincaré inequalities in fractional Sobolev spaces*, Ann. Acad. Sci. Fenn. Math., 43(2):885–903, 2018.
- [22] Z. Du and H. Duan, *A mixed method for Maxwell eigenproblem*, J. Sci. Comput. 82(1), paper no. 8, 37pp., 2020.
- [23] H. Duan, Z. Du, W. Liu and S. Zhang. *New Mixed Elements for Maxwell Equations*, SIAM J. Numer. Anal., 57(1):320–54, 2019.
- [24] H. Duan, W. Liu, J. Ma, R.C.E. Tan, and S. Zhang, *A family of optimal Lagrange elements for Maxwell’s equations*, J. Comput. Appl. Math., 358:241–265, 2019.
- [25] T. Dupont and R. Scott, *Polynomial approximation of functions in Sobolev spaces*, Math. Comp. 34:441–463, 1980.
- [26] A. Ern and J.-L. Guermond, *Finite element quasi-interpolation and best approximation*, ESAIM: Mathematical Modelling and Numerical Analysis, 51(4):1367–85, 2017.
- [27] R. Falk and M. Neilan, *Stokes complexes and the construction of stable finite element methods with pointwise mass conservation*, SIAM J. Numer. Anal., 51(2):1308–1326, 2013.
- [28] G. Fu, J. Guzmán, and M. Neilan, *Exact smooth piecewise polynomial sequences on Alfeld splits*, Math. Comp., 89(323):1059–1091, 2020.
- [29] J. Guzmán, A. Lischke, and M. Neilan, *Exact sequences on Powell–Sabin splits*, Calcolo, 57(13), 2020.
- [30] J. Guzmán, A. Lischke, and M. Neilan, *Exact sequences on Worsey–Farin splits*, arXiv:2008.05431, 2020.
- [31] J. Guzmán and R. Scott, *The Scott–Vogelius finite elements revisited*, Math. Comp., 88(316):515–529, 2019.

- [32] T. Kato, *Perturbation theory for linear operators*, Reprint of the 1980 edition. Classics in Mathematics. Springer-Verlag, Berlin, 1995.
- [33] F. Kikuchi, *On a discrete compactness property for the Nédélec finite elements*, J. Faculty of Science, U. Tokyo. Sect. 1 A, Mathematics, 36 (3), 479–490, 1989.
- [34] M.-J. Lai and L. L. Schumaker, *Spline functions on triangulations*, Encyclopedia of Mathematics and its Applications, 110., Cambridge University Press, Cambridge, 2007
- [35] M. Neilan, *The Stokes Complex: A review of exactly divergence-free finite element pairs for incompressible flows*, 75 Years of Mathematics of Computation, Contemporary Mathematics, volume 754, AMS, to appear.
- [36] JC Nédélec, *Mixed finite elements in \mathbb{R}^3* , Numerische Mathematik. 1980 Sep 1;35(3):315–41.
- [37] JC Nédélec, *A new family of mixed finite elements in \mathbb{R}^3* , Numerische Mathematik. 1986 Jan 1;50(1):57–81.
- [38] M. J. D. Powell and M. A. Sabin, *Piecewise quadratic approximations on triangles*, ACM Trans. Math. Software 3(4):316–325, 1977.
- [39] J. Qin, *On the convergence of some low order mixed finite elements for incompressible fluids*, Ph.D. Thesis, The Pennsylvania State University, 1994.
- [40] L. R. Scott and M. Vogelius, *Norm estimates for a maximal right inverse of the divergence operator in spaces of piecewise polynomials*, RAIRO Model. Math. Anal. Numer. 19(1):111–143, 1985.
- [41] L. R. Scott and S. Zhang, *Finite element interpolation of non smooth functions satisfying boundary conditions*, Math. Comp., 54(190):483–493, 1990.
- [42] S. H. Wong and Z. J. Cendes, *Combined finite element-modal solution of three-dimensional eddy current problems*, IEEE Transactions on Magnetics, 24(6):2685–2687, 1988.
- [43] S. Zhang, *A new family of stable mixed finite elements for the 3D Stokes equations* Mathematics of computation. 2005;74(250):543–54.

APPENDIX A. PROOF OF LEMMA 3.1

In order to describe the new interpolant, we first remind the reader of the Scott-Zhang interpolant [41]. For every $z \in \mathcal{V}_h$ we define $\phi_z \in \mathcal{P}_1^c(\mathcal{T}_h)$ to be the hat function $\phi_z(y) = \delta_{yz}$ for all $y \in \mathcal{V}_h$. Also for every $z \in \mathcal{V}_h$, we identify an arbitrary edge e_z of the mesh that contains z with the only constraint that e_z is a boundary edge if z is a boundary vertex. Then there exists function $\psi_z \in L^\infty(e_z)$ such that

$$(A.1) \quad \int_{e_z} \psi_z \phi_y = \delta_{yz} \quad y \in \mathcal{V}_h.$$

Moreover,

$$(A.2) \quad \|\psi_z\|_{L^\infty(e_z)} \leq \frac{C}{|e_z|}.$$

The Scott-Zhang interpolant $\tilde{\mathbf{I}}_h$ is given by:

$$(A.3) \quad \tilde{\mathbf{I}}_h \boldsymbol{\tau}(x) = \sum_{z \in \mathcal{V}_h} \left(\int_{e_z} \psi_z \boldsymbol{\tau} \right) \phi_z(x).$$

Although the Scott-Zhang interpolant has the approximation properties we need, it might not preserve the tangential trace to be zero. More precisely, if $\boldsymbol{\tau} \in \mathbf{H}^{\frac{1}{2}+\delta}(\Omega) \cap \mathbf{H}_0(\text{rot}; \Omega)$ then $\tilde{\mathbf{I}}_h \boldsymbol{\tau} \cdot \mathbf{t}$ might not vanish on edges that touch a corner vertex. Therefore, we must modify the Scott-Zhang interpolant on such vertices.

For every corner boundary vertex $z \in \mathcal{V}_h^C$ we will consider the two boundary edges, e_z^1, e_z^2 , that that have z as an endpoint. We let \mathbf{n}_z^i be the outward pointing normal to e_z^i and \mathbf{t}_z^i the tangent vector to \mathbf{n}_z^i that is rotated 90 degrees counterclockwise. We then have the existence of $\psi_z^i \in L^\infty(e_z^i)$ such that

$$(A.4) \quad \int_{e_z^i} \psi_z^i \phi_y = \delta_{yz} \quad y \in \mathcal{V}_h,$$

$$(A.5) \quad \|\psi_z^i\|_{L^\infty(e_z^i)} \leq \frac{C}{|e_z^i|}.$$

We can then define the modified Scott-Zhang interpolant as follows:

$$(A.6) \quad \mathbf{I}_h \boldsymbol{\tau}(x) := \sum_{z \in \mathcal{V}_h \setminus \mathcal{V}_h^C} \left(\int_{e_z} \psi_z \boldsymbol{\tau} \right) \phi_z(x) + \sum_{z \in \mathcal{V}_h^C} \boldsymbol{\beta}_z(\boldsymbol{\tau}) \phi_z(x),$$

where

$$\boldsymbol{\beta}_z(\boldsymbol{\tau}) := \frac{\mathbf{n}_z^2}{\mathbf{n}_z^2 \cdot \mathbf{t}_z^1} \int_{e_z^1} (\boldsymbol{\tau} \cdot \mathbf{t}_z^1) \psi_z^1 + \frac{\mathbf{n}_z^1}{\mathbf{n}_z^1 \cdot \mathbf{t}_z^2} \int_{e_z^2} (\boldsymbol{\tau} \cdot \mathbf{t}_z^2) \psi_z^2.$$

We now proceed to prove Lemma 3.1 in four steps.

(i) $\mathbf{I}_h : \mathbf{H}^{\frac{1}{2}+\delta}(\Omega) \cap \mathbf{H}_0(\text{rot}; \Omega) \rightarrow \mathcal{P}_1^c(\mathcal{T}_h) \cap \mathbf{H}_0(\text{rot}, \Omega)$: If $\boldsymbol{\tau} \in \mathbf{H}^{\frac{1}{2}+\delta}(\Omega) \cap \mathbf{H}_0(\text{rot}; \Omega)$, then clearly $\mathbf{I}_h \boldsymbol{\tau}(z) = 0$ for every $z \in \mathcal{V}_h^C$. Also we have $\mathbf{I}_h \boldsymbol{\tau}(z) \cdot \mathbf{t}_z = 0$ for all $z \in \mathcal{V}_h \setminus \mathcal{V}_h^C$ where \mathbf{t}_z is tangent to e_z . Thus we have that $\mathbf{I}_h \boldsymbol{\tau} \cdot \mathbf{t} = 0$ on $\partial\Omega$.

(ii) \mathbf{I}_h is a projection: In order to show it is a projection we need to show that $\mathbf{I}_h \boldsymbol{\tau}(z) = \boldsymbol{\tau}(z)$ for all $z \in \mathcal{V}_h$ and $\boldsymbol{\tau} \in \mathcal{P}_1^c(\mathcal{T}_h)$. To this end, let $\boldsymbol{\tau} \in \mathcal{P}_1^c(\mathcal{T}_h)$. If $z \in \mathcal{V}_h \setminus \mathcal{V}_h^C$ then $\mathbf{I}_h \boldsymbol{\tau}(z) = \int_{e_z} \psi_z \boldsymbol{\tau}$. However, $\int_{e_z} \psi_z \boldsymbol{\tau} = \boldsymbol{\tau}(z)$ by (A.1), since $\boldsymbol{\tau}|_{e_z} = \boldsymbol{\tau}(z) \phi_z + \boldsymbol{\tau}(y) \phi_y$ where y is the other end point of e_z . On the other hand, if $z \in \mathcal{V}_h^C$ then $\mathbf{I}_h \boldsymbol{\tau}(z) = \boldsymbol{\beta}_z(\boldsymbol{\tau})$. Then, we have $\boldsymbol{\beta}_z(\boldsymbol{\tau}) \cdot \mathbf{t}_z^i = \int_{e_z^i} (\boldsymbol{\tau} \cdot \mathbf{t}_z^i) \psi_z^i$. Using (A.1) we have that $\int_{e_z^i} (\boldsymbol{\tau} \cdot \mathbf{t}_z^i) \psi_z^i = \boldsymbol{\tau}(z) \cdot \mathbf{t}_z^i$. Thus we have shown that $\mathbf{I}_h \boldsymbol{\tau}(z) \cdot \mathbf{t}_z^i = \boldsymbol{\tau}(z) \cdot \mathbf{t}_z^i$ for $i = 1, 2$ and thus $\mathbf{I}_h \boldsymbol{\tau}(z) = \boldsymbol{\tau}(z)$.

(iii) *Stability estimate*: We derive a stability estimate following the arguments of [41, 16]. First we note that by an inverse estimate we have

$$|\mathbf{I}_h \boldsymbol{\tau}|_{H^{\frac{1}{2}+\delta}(T)} \leq Ch_T^{-\frac{1}{2}-\delta} \|\mathbf{I}_h \boldsymbol{\tau}\|_{L^2(T)}.$$

Thus, we only need to bound the L^2 -norm. To do this, we first note the trace inequality (cf. [16, Proposition 3.1])

$$\|\boldsymbol{\tau}\|_{L^1(e_z)} \leq C(\|\boldsymbol{\tau}\|_{L^2(T)} + h_T^{\frac{1}{2}+\delta} |\boldsymbol{\tau}|_{H^{\frac{1}{2}+\delta}(T)}),$$

for $T \in \mathcal{T}_h$ with $e_z \subset \partial T$. We remind the reader that the number of corner points \mathcal{V}_h^C is finite and independent of the mesh \mathcal{T}_h and hence $M := \max_{z \in \mathcal{V}_h^C} \frac{1}{\mathbf{n}_z^1 \cdot \mathbf{t}_z^2}$ is finite. Thus, using (A.2) and (A.5), we have

$$\begin{aligned} \|\mathbf{I}_h \boldsymbol{\tau}\|_{L^2(T)} &\leq \sum_{\substack{z \in \mathcal{V}_h \setminus \mathcal{V}_h^C \\ z \in \bar{T}}} \|\phi_z\|_{L^2(T)} \|\psi_z\|_{L^\infty(e_z)} \|\boldsymbol{\tau}\|_{L^1(e_z)} \\ &\quad + M \sum_{\substack{z \in \mathcal{V}_h^C \\ z \in \bar{T}}} \|\phi_z\|_{L^2(T)} (\|\psi_z^1\|_{L^\infty(e_z^1)} \|\boldsymbol{\tau}\|_{L^1(e_z^1)} + \|\psi_z^2\|_{L^\infty(e_z^2)} \|\boldsymbol{\tau}\|_{L^1(e_z^2)}) \\ &\leq C(1+M) (\|\boldsymbol{\tau}\|_{L^2(\omega(T))} + h_T^{\frac{1}{2}+\delta} |\boldsymbol{\tau}|_{H^{\frac{1}{2}+\delta}(\omega(T))}), \end{aligned}$$

where we used that $\|\phi_z\|_{L^2(T)} \leq Ch_T$. Hence, combing the above results we obtain

$$(A.7) \quad h_T^{\frac{1}{2}+\delta} |\mathbf{I}_h \boldsymbol{\tau}|_{H^{\frac{1}{2}+\delta}(T)} + \|\mathbf{I}_h \boldsymbol{\tau}\|_{L^2(T)} \leq C(1+M) (\|\boldsymbol{\tau}\|_{L^2(\omega(T))} + h_T^{\frac{1}{2}+\delta} |\boldsymbol{\tau}|_{H^{\frac{1}{2}+\delta}(\omega(T))}).$$

(iv) *Estimate (3.1)*: Let $\mathbf{w} = \frac{1}{|\omega(T)|} \int_{\omega(T)} \boldsymbol{\tau}$, we have that

$$(A.8) \quad \|\boldsymbol{\tau} - \mathbf{w}\|_{L^2(\omega(T))} \leq Ch_T^{\frac{1}{2}+\delta} |\boldsymbol{\tau}|_{H^{\frac{1}{2}+\delta}(\omega(T))}.$$

The estimate (A.8) for $\delta = \frac{1}{2}$ is shown in [41, Section 4]. The estimate (A.8) for $\delta \in (0, \frac{1}{2})$ can be found for example in [21, Proposition 2.1] and [7, Lemma 3.1]. See also [26, Lemma 5.6].

Because \mathbf{w} is constant we have that $\mathbf{I}_h \mathbf{w} = \mathbf{w}$ on T , and thus using (A.7) and (A.8) we obtain

$$\begin{aligned} \|\mathbf{I}_h \boldsymbol{\tau} - \boldsymbol{\tau}\|_{L^2(T)} &= \|\mathbf{I}_h(\boldsymbol{\tau} - \mathbf{w}) + (\mathbf{w} - \boldsymbol{\tau})\|_{L^2(T)} \\ &\leq C(1 + M)(\|\boldsymbol{\tau} - \mathbf{w}\|_{L^2(\omega(T))} + h_T^{\frac{1}{2}+\delta} |\boldsymbol{\tau}|_{H^{\frac{1}{2}+\delta}(\omega(T))}) \\ &\leq C(1 + M)(h_T^{\frac{1}{2}+\delta} |\boldsymbol{\tau}|_{H^{\frac{1}{2}+\delta}(\omega(T))}). \end{aligned}$$

Similarly, $|\mathbf{I}_h \boldsymbol{\tau}|_{H^{\frac{1}{2}+\delta}(T)} = |\mathbf{I}_h \boldsymbol{\tau} - \mathbf{w}|_{H^{\frac{1}{2}+\delta}(T)} = |\mathbf{I}_h(\boldsymbol{\tau} - \mathbf{w})|_{H^{\frac{1}{2}+\delta}(T)}$ and one can use (A.7) and (A.8) again to get $|\mathbf{I}_h \boldsymbol{\tau}|_{H^{\frac{1}{2}+\delta}(T)} \leq C(1 + M) |\boldsymbol{\tau}|_{H^{1/2+\delta}(\omega(T))}$. This completes the proof of Lemma 3.1.

KING ABDULLAH UNIVERSITY OF SCIENCE AND TECHNOLOGY, SAUDI ARABIA AND UNIVERSITY OF PAVIA, ITALY
Email address: daniele.boffi@kaust.edu.sa

DIVISION OF APPLIED MATHEMATICS, BROWN UNIVERSITY
Email address: johnny_guzman@brown.edu

DEPARTMENT OF MATHEMATICS, UNIVERSITY OF PITTSBURGH
Email address: neilan@pitt.edu